

15th CEAS-ASC Workshop
1st Scientific Workshop of X-NOISE EV
Acoustic Liners and Associated Propagation Techniques
EPFL, Lausanne
October 13-14, 2011



Computational tools for modeling acoustic liners and propagation:

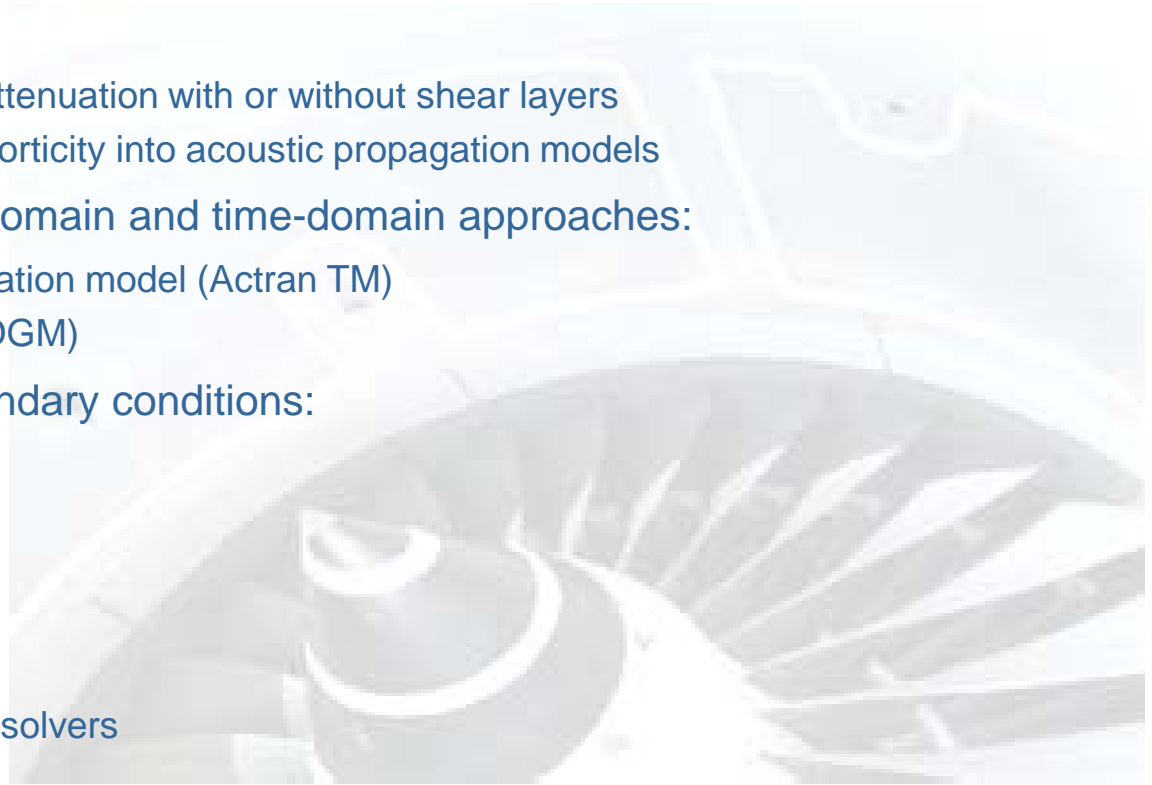
Review of some key ingredients and challenges

J.P. Coyette, Y. Detandt, G. Lielens and C. Legendre

Free Field Technologies, Belgium

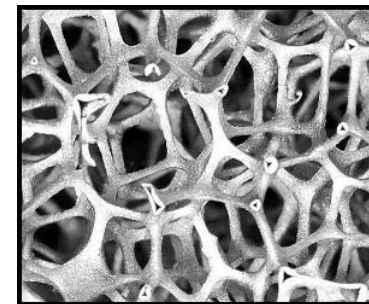
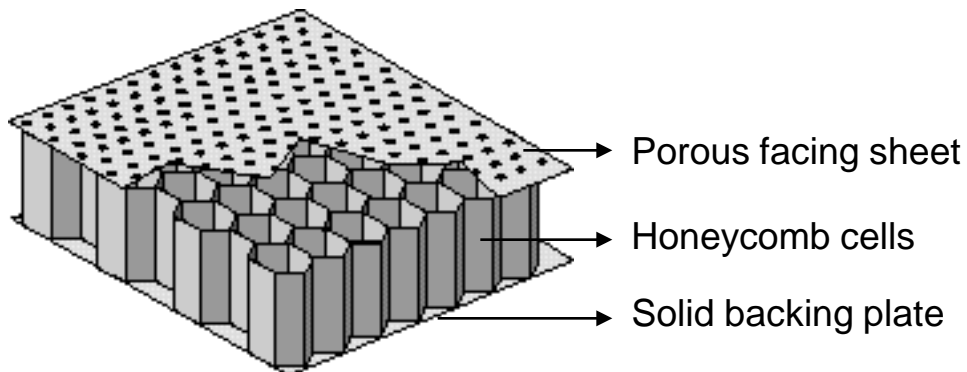
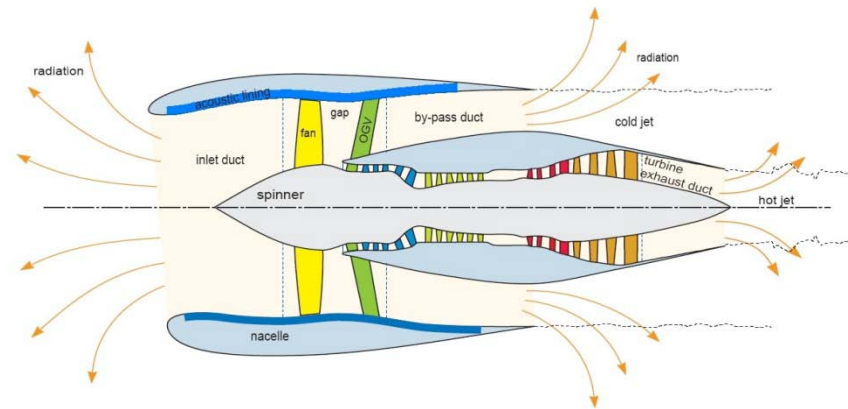
Summary

- ➔ Modeling acoustic treatments
- ➔ Acoustic propagation with flow
- ➔ Flow conditions:
 - Assessing acoustic attenuation with or without shear layers
 - Incorporating or not vorticity into acoustic propagation models
- ➔ Alternative frequency-domain and time-domain approaches:
 - Convected wave equation model (Actran TM)
 - LEE model (Actran DGM)
- ➔ Modeling radiation boundary conditions:
 - Infinite elements
 - Buffer zones
- ➔ Modal duct excitations
- ➔ Software requirements:
 - Parallelism and HPC solvers
 - Energy indicators
- ➔ Next challenges



Context

- ➔ Various aircraft noise sources
- ➔ Fan noise = dominant component at take-off/landing for HBPR turbofan engines
- ➔ Attenuation using liners (engine intake, exhaust ducts)
- ➔ Typical (locally reacting) acoustic liners:
 - SDOF
 - DDOF or MDOF
- ➔ Need for efficient models incorporating liners:
 - Extended frequency range
 - Non-uniform treatments
 - Adaptive liners
 - New absorbing materials (bulk reacting)
 - Optimization



Metal foam

Noise reduction technologies

➔ Liners and noise reduction technologies:

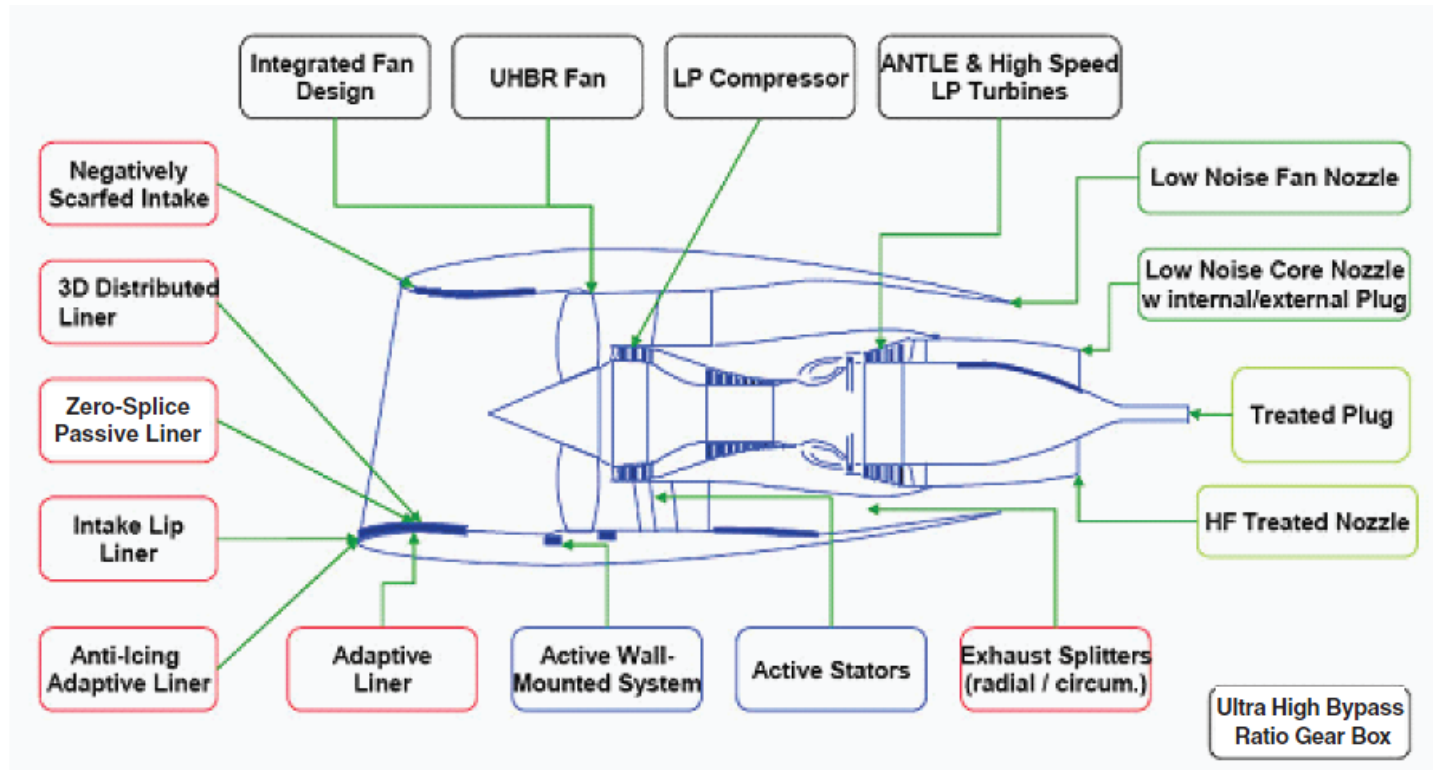


FIGURE 5-9 Engine/nacelle noise reduction technologies. UHBR = ultra high bypass ratio. Source: SBAC (2009).

(from « Technology for a Quieter America », National Academy of Engineering, 2010)

Modeling liners

➞ Locally reacting liners:

▪ Frequency domain:

- No flow case:

$$p(\omega) = z(\omega) v_n(\omega)$$

- Flow case (Myers):

$$v_n(\omega) = \frac{p(\omega)}{z(\omega)} + v_0 \cdot \nabla \left(\frac{p(\omega)}{i\omega z(\omega)} \right) - \frac{p(\omega)}{i\omega z(\omega)} n \cdot (n \cdot \nabla v_0)$$

▪ Time domain:

- Convolution integral:

$$p(t) = \frac{1}{2\pi} \int_{-\infty}^{+\infty} z(t-\tau) v_n(\tau) d\tau$$

▪ Comments:

- Emergence of refined (DNS) models for predicting impedance (Zhang-Codony)
- Stability issues of Myers boundary condition (*)
- Need for stable/causal $z(t)$ models (Tam-Auriault, Ozyoruk-Long, Richter, etc)

➞ Non-locally reacting (or bulk reacting) liners:

- More advanced models (Biot for porous materials)

(*) see Brambley (AIAA paper 2010-3942) for improved Myers bc

Modeling acoustic propagation with flow

➔ LEE model (unknowns = p' , v' and ρ') ← Actran DGM

$$\frac{\partial \rho'}{\partial t} + \nabla \cdot (\rho' v_0 + \rho_0 v') = 0$$

$$\rho_0 \left(\frac{\partial}{\partial t} + v_0 \cdot \nabla \right) v' + \rho_0 (v' \cdot \nabla) v_0 + \rho' (v_0 \cdot \nabla) v_0 + \nabla p' = 0$$

$$\left(\frac{\partial}{\partial t} + v_0 \cdot \nabla \right) p' + v' \cdot \nabla p_0 + \gamma p_0 (\nabla \cdot v') + \gamma p' (\nabla \cdot v_0) = 0$$

➔ Convected Wave Equation model (unknown = ϕ') ← Actran TM

$$p' = c_0^2 \rho' = -\rho_0 \left(\frac{\partial}{\partial t} + v_0 \cdot \nabla \right) \phi'$$

$$\frac{D}{Dt} \left(\frac{\rho_0}{c_0^2} \frac{D\phi'}{Dt} \right) - \nabla \cdot (\rho_0 \nabla \phi') = 0$$

Further assumptions:

- Homentropic case
- Irrotational flow

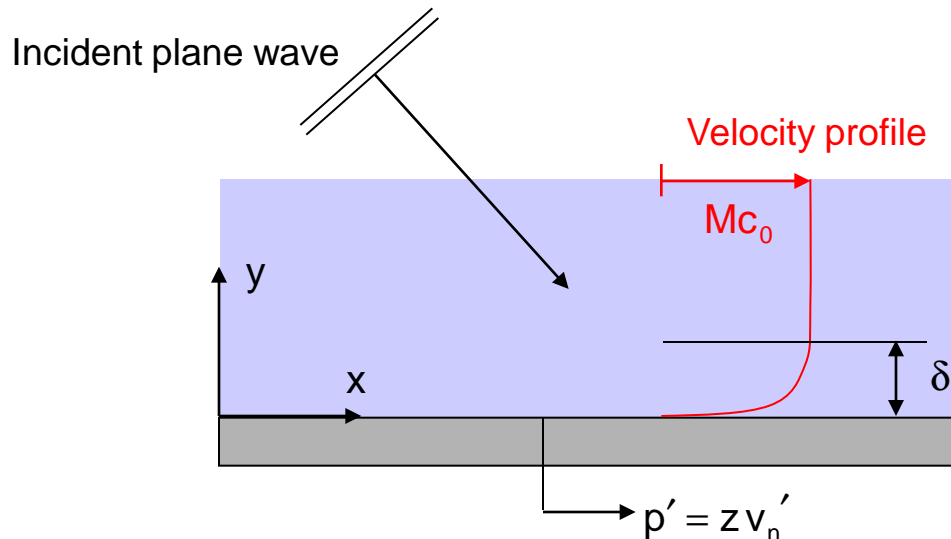
➔ Main issues:

- Model sizes (LEE – 4 or 5 dofs/node, CWE – 1 dof/node)
- Effect of boundary layers on acoustic propagation/attenuation?



Evaluation of propagation models

- ➔ Context: evaluation of the reflection coefficient along a treated surface
- ➔ Objective: assessment of boundary layer thickness (δ) and flow velocity (M)
- ➔ Models:
 - Pridmore-Brown model (1958) → reference
 - Myers model (1980) → valid for an infinitely thin boundary layer
 - Möhring model (1999) and extended Möhring models → valid for a rotational flow
 - Convected wave equation (velocity potential) → valid for an irrotational flow



$$\mathbf{v}_0 = \begin{pmatrix} U(y) \\ 0 \\ 0 \end{pmatrix}$$

Pridmore-Brown model

- ➔ Assumption of a sheared flow along x only + propagating wave along x:

$$\mathbf{v}_0^T = (U(y) \quad 0 \quad 0)$$

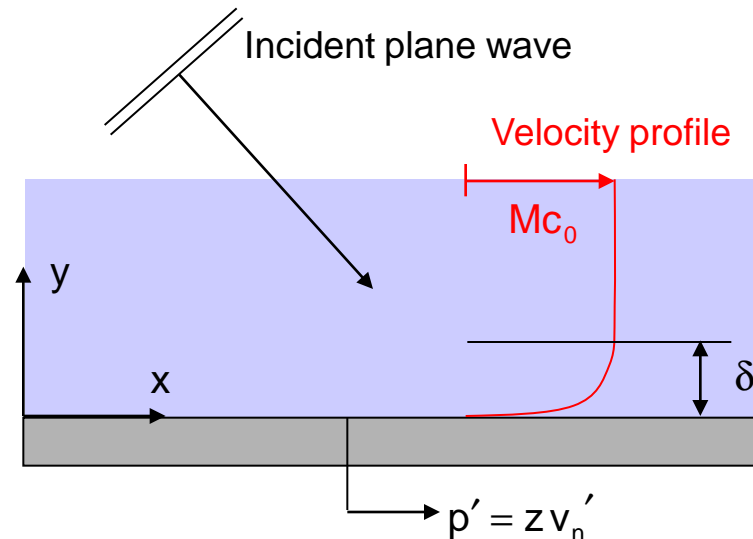
$$p'(x, y, \omega) = p'(y) e^{-ik_x x} e^{+i\omega t}$$

- ➔ Reference (exact!) model for this kind of flow:

$$\frac{d^2 p'}{dy^2} + \frac{2k_x}{k - Mk_x} \frac{dM}{dy} \frac{dp'}{dy} + k^2 \left(1 - \frac{k_x^2}{k^2} (1 - M^2) - 2M \frac{k_x}{k} \right) p' = 0$$

- ➔ Notations:

- Mach number M
- Wavenumber k
- Spatial wavenumber k_x
- Pressure p'



$$\mathbf{v}_0 = \begin{pmatrix} U(y) \\ 0 \\ 0 \end{pmatrix}$$



Möhring model

➔ (Improved) Möhring model (in terms of total enthalpy B'):

$$\frac{\partial}{\partial t} \left(\frac{\rho_0}{\rho_T c^2} \frac{DB'}{Dt} \right) + \nabla \cdot \left(\frac{\rho_0 v_0}{\rho_T c^2} \frac{DB'}{Dt} + \frac{\rho_0}{\rho_T^2} \Phi \nabla B' \right) = 0 \quad \longrightarrow \quad \begin{aligned} p' &= f(B') \\ v' &= g(B') \end{aligned}$$

➔ Notations:

- « Rotational » material derivative:

$$\frac{DB'}{Dt} = \frac{\partial B'}{\partial t} + (v_0 + \chi_0) \cdot \nabla B'$$

- « Rotational » velocity associated with acoustic phenomena:

$$\chi_0 = \Omega_0^T \cdot (\omega_0 \times v_0)$$

$$\begin{aligned} \Phi &= \Theta_0 \Omega_0 - I \\ \Omega_0 &= (\Theta_0 - i\omega I)^{-1} \end{aligned} \quad \Theta_0 = \begin{bmatrix} 0 & +\omega_z & -\omega_y \\ -\omega_z & 0 & +\omega_x \\ +\omega_y & -\omega_x & 0 \end{bmatrix} \quad \omega_0 = \nabla \times v_0 = \begin{pmatrix} \omega_x \\ \omega_y \\ \omega_z \end{pmatrix}$$

Reference: C. Legendre and G. Lielens, internal report, FFT, 2011

Möhring model / Numerical stability

➔ Stability of Möhring model:

$$\Omega_0^{-1} = \begin{bmatrix} -i\omega & +\omega_z & -\omega_y \\ -\omega_z & -i\omega & +\omega_x \\ +\omega_y & -\omega_x & -i\omega \end{bmatrix} \quad \nabla \times \mathbf{v}_0 = \begin{pmatrix} \omega_x \\ \omega_y \\ \omega_z \end{pmatrix}$$

➔ Evaluation of velocity field \mathbf{v}' requires the inversion of this matrix so that

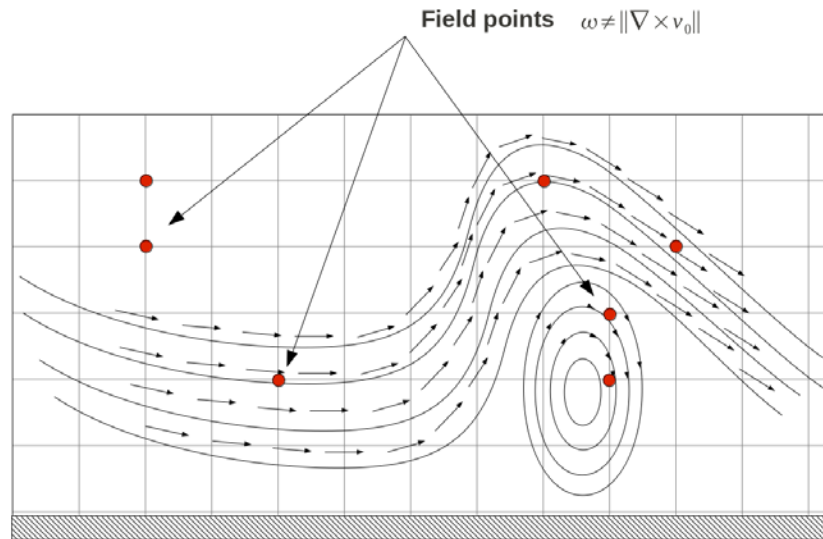
$$\det(\Omega_0^{-1}) \neq 0 \quad \Leftrightarrow \quad +i\omega^3 - i\omega(\omega_x^2 + \omega_y^2 + \omega_z^2) \neq 0$$

➔ Instability occurs when

- $\omega = 0 \rightarrow$ zero frequency
- $\omega_x^2 + \omega_y^2 + \omega_z^2 = \omega^2 \rightarrow$ magnitude of vorticity vector = angular frequency

Need for a stabilization procedure

- ➔ Existence of singular points in a rotational flow:



Occurrence of points where $\omega_x^2 + \omega_y^2 + \omega_z^2 = \omega^2$

- ➔ Need for a stabilization procedure

Regularization procedure

➔ Introduction of vorticity damping:

$$\Omega_0^{-1} = (1 + i\varepsilon) \Theta_0 - i\omega I$$

or

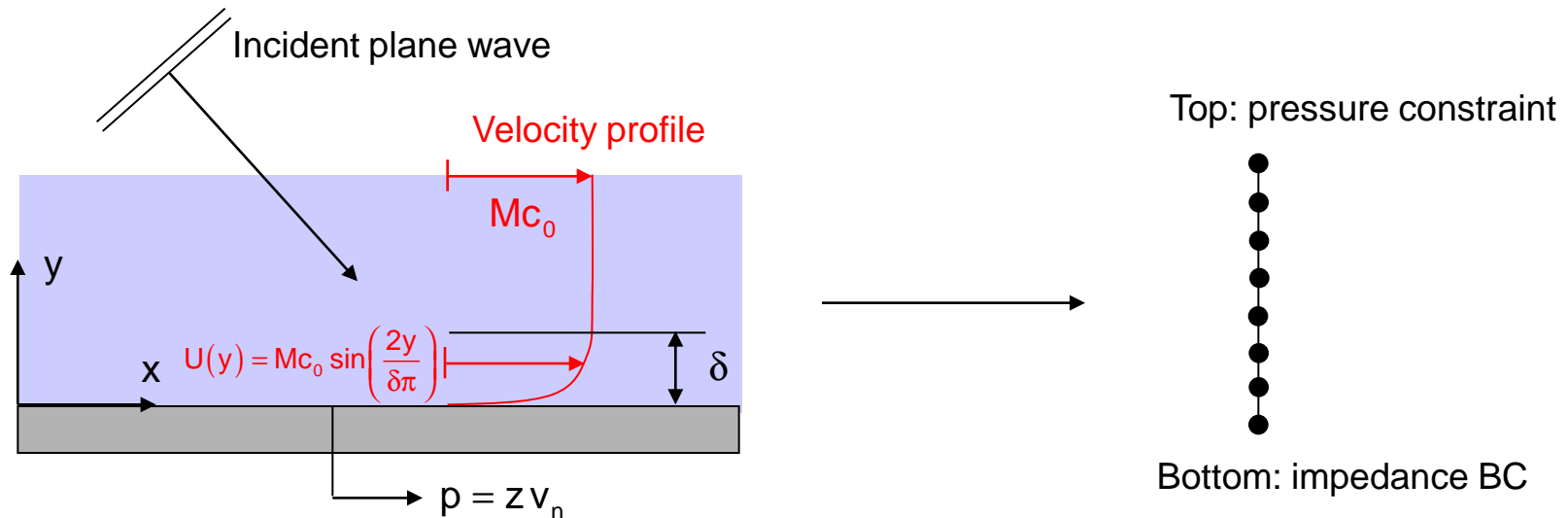
$$\Omega_0^{-1} = \begin{bmatrix} -i\omega & +\omega_z (1 + i\varepsilon) & -\omega_y (1 + i\varepsilon) \\ -\omega_z (1 + i\varepsilon) & -i\omega & +\omega_x (1 + i\varepsilon) \\ +\omega_y (1 + i\varepsilon) & -\omega_x (1 + i\varepsilon) & -i\omega \end{bmatrix} \quad \nabla \times \mathbf{v}_0 = \begin{pmatrix} \omega_x \\ \omega_y \\ \omega_z \end{pmatrix}$$

➔ Selection of ε value:

- Stability requirement: ε should be real
- Accuracy requirement: low ε value (typically ... 0.01 ...)

Evaluation of the reflection coefficient

➔ Selection of a 1-D FE model:



➔ Material properties:

- Air with usual properties ($c_0 = 340$ m/s, $\rho_0 = 1.225$ kg/m³)
- Impedance: $z = \rho_0 c_0 (0.5 + 0.1i)$

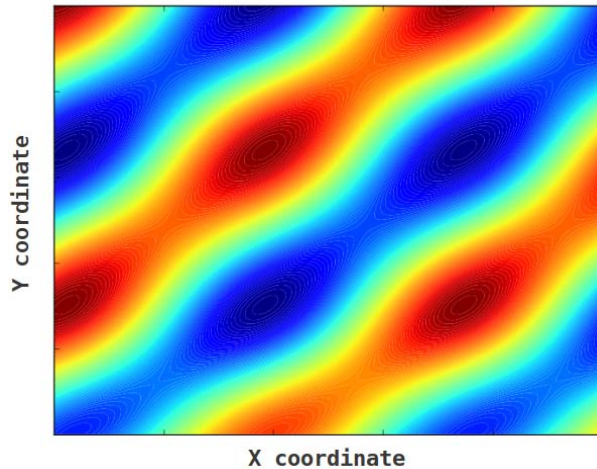
➔ Range of input data:

- Mach number M : 0.01 – 1 (-)
- Vorticity damping ε : 0.1 – 1 (-)
- Incidence angle: 0 – 90 (degrees)
- Frequency: 1-10000 (Hz)

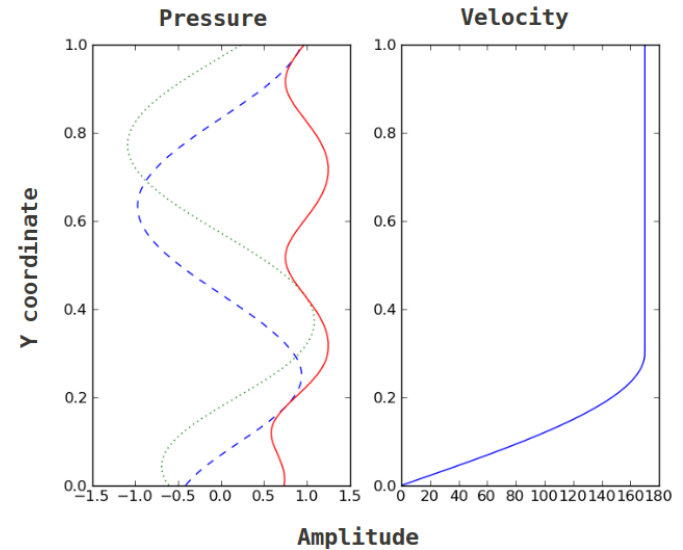
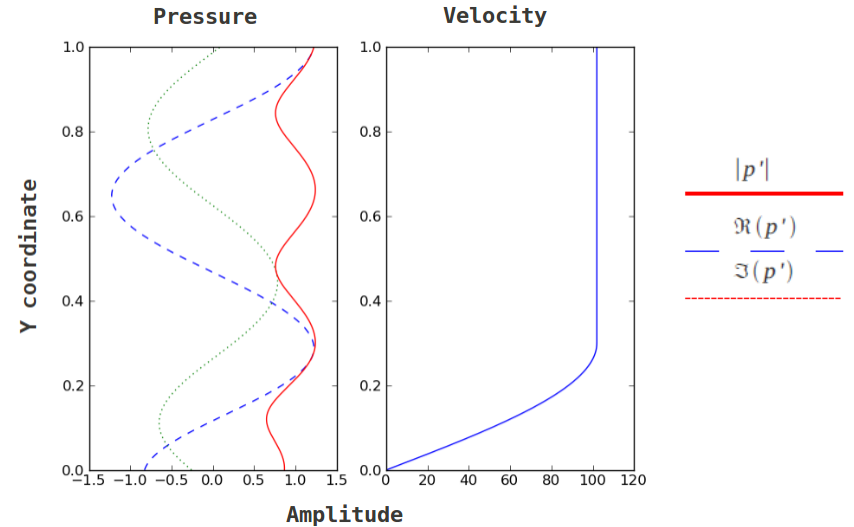
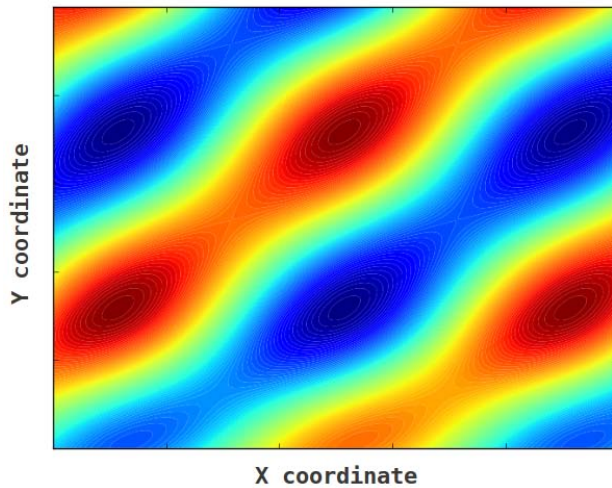
Numerical results (PMB)

➤ Pridmore-Brown equation:

Pressure map (800 Hz, Ma=0.3)

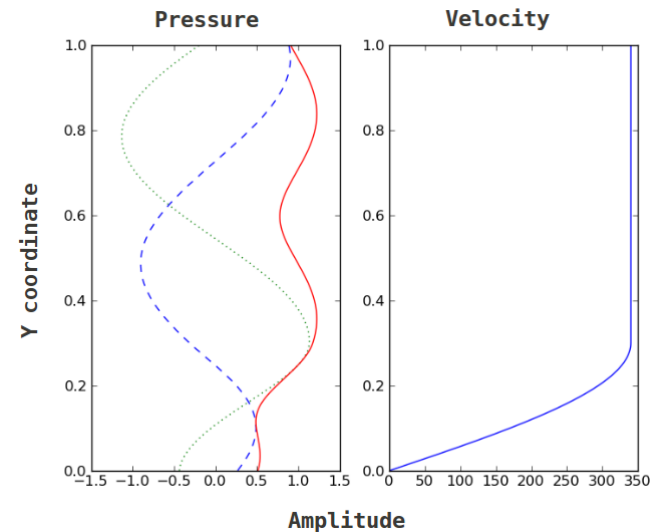
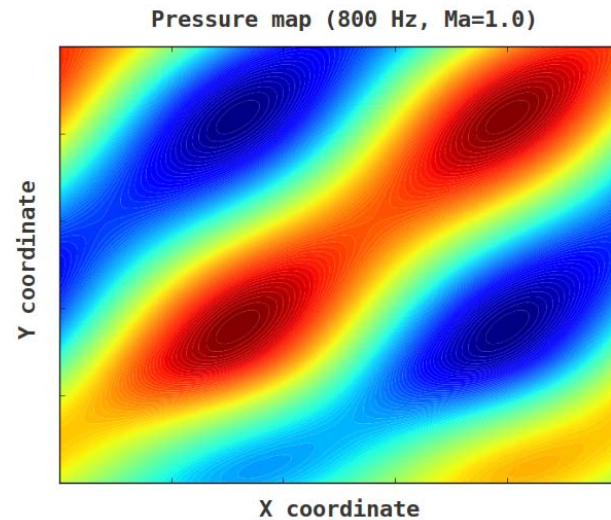
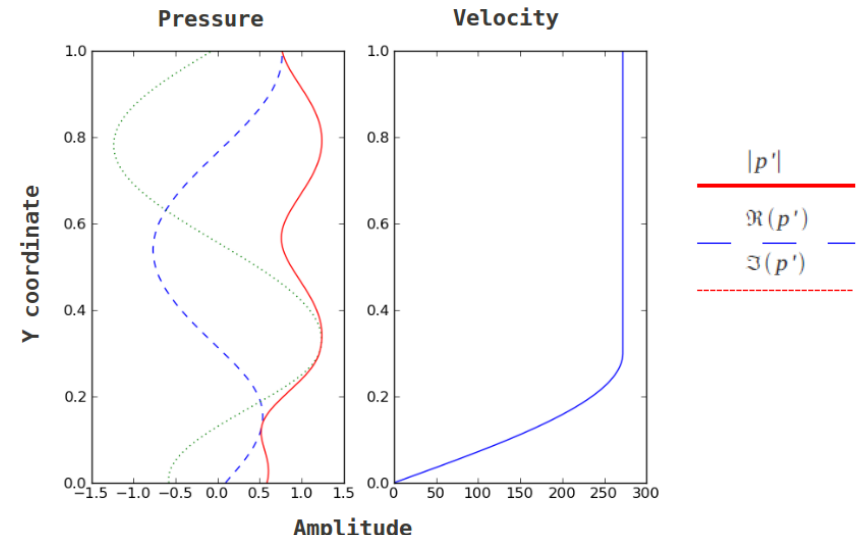
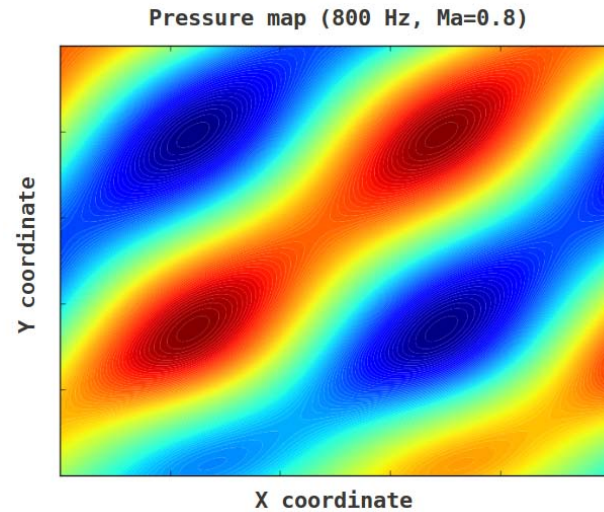


Pressure map (800 Hz, Ma =0.5)



Numerical Results (PMB)

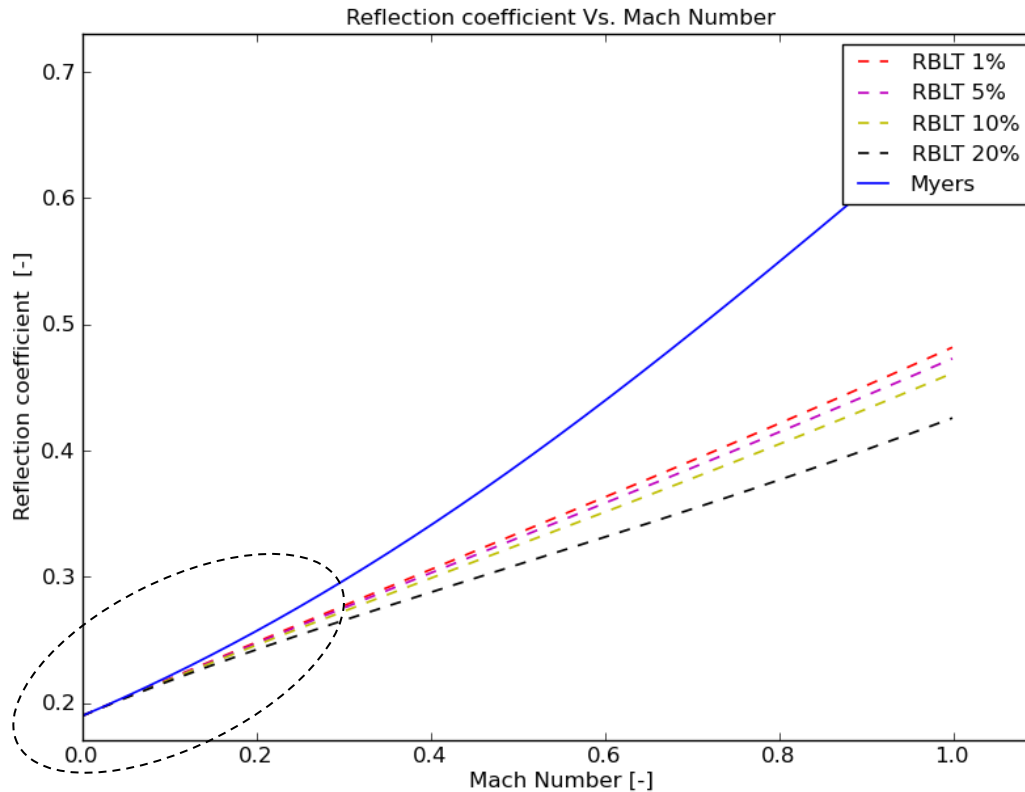
➔ Pridmore-Brown equation:



Numerical results (Myers vs. PMB)

➤ Myers vs. Pridmore-Brown model:

➤ Reflection coefficient vs. Mach number



Myers \approx Pridmore-Brown

$$\left| \begin{array}{l} \text{RBLT} = \frac{\delta}{\lambda_0} \rightarrow 0 \\ \text{Low } M \end{array} \right.$$

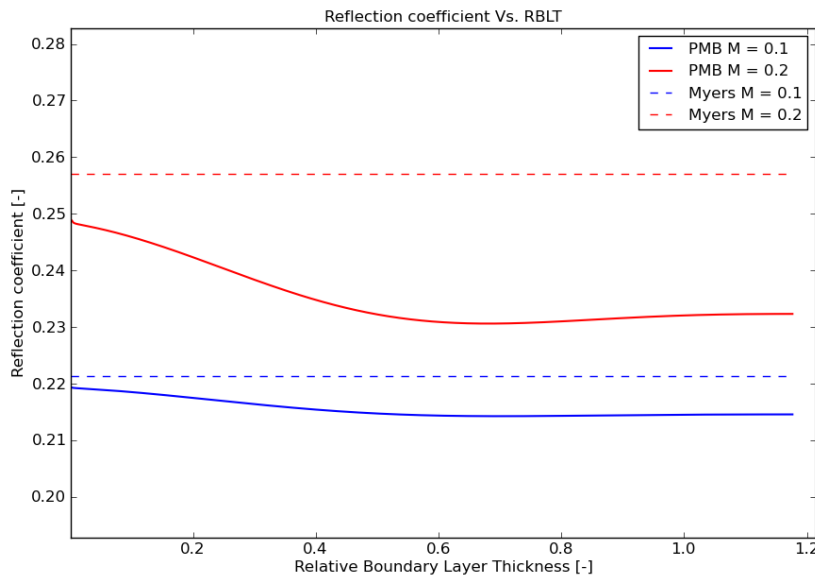
Numerical results (Myers vs. PMB)

➤ Myers vs. Pridmore-Brown model:

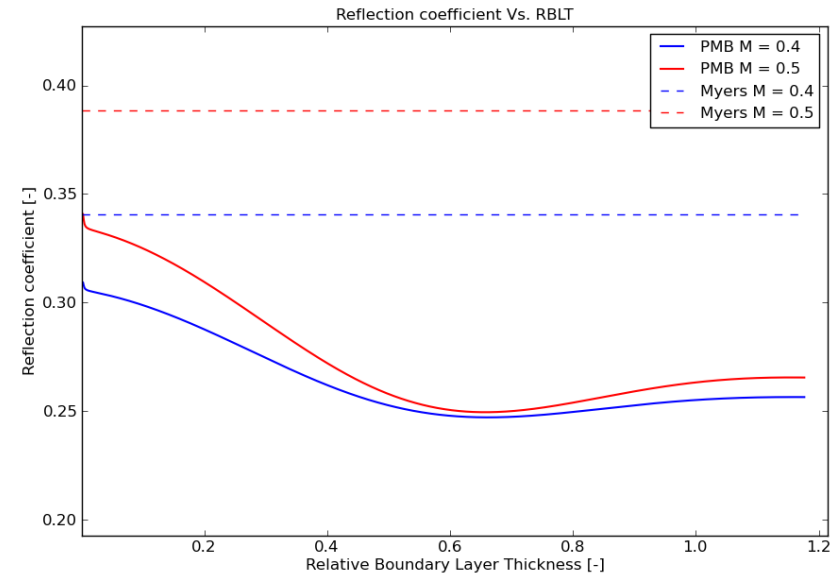
➤ Reflection coefficient vs. relative boundary layer thickness (RBLT)

Myers \approx Pridmore-Brown

$$\left| \begin{array}{l} \text{RBLT} = \frac{\delta}{\lambda_0} \rightarrow 0 \\ \text{Low } M \end{array} \right.$$



Ma = 0.1 - 0.2



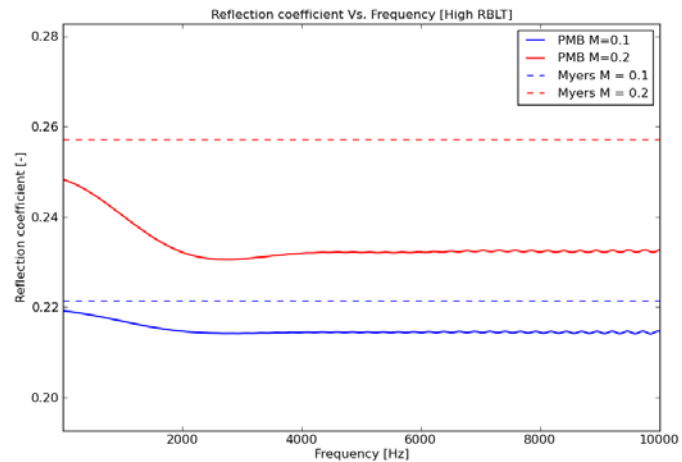
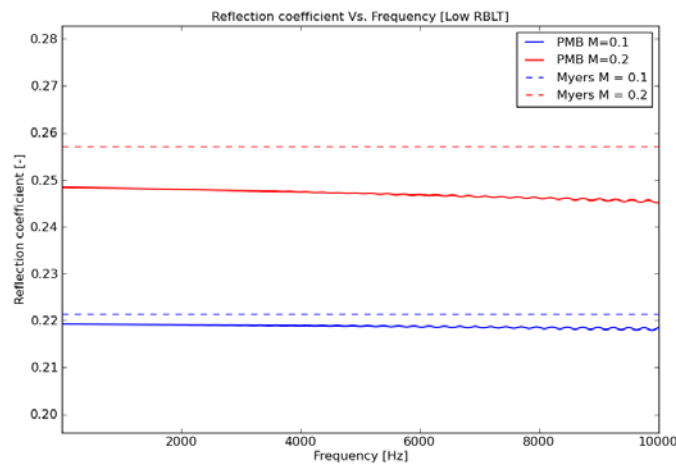
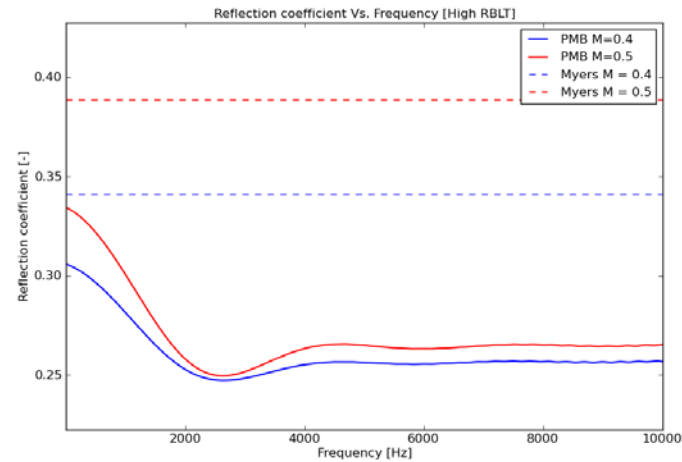
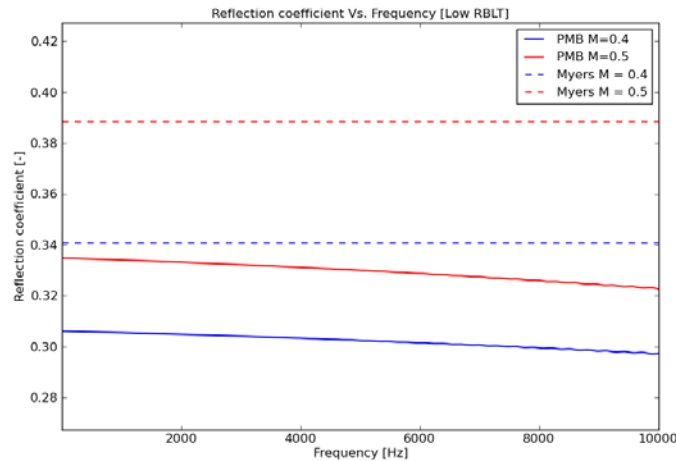
Ma = 0.4 - 0.5

Numerical results (Myers vs. PMB)



Myers vs. Pridmore-Brown model:

Mach Number

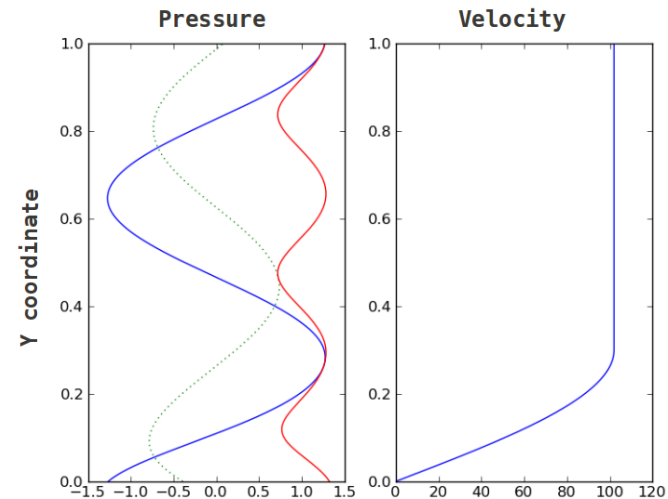
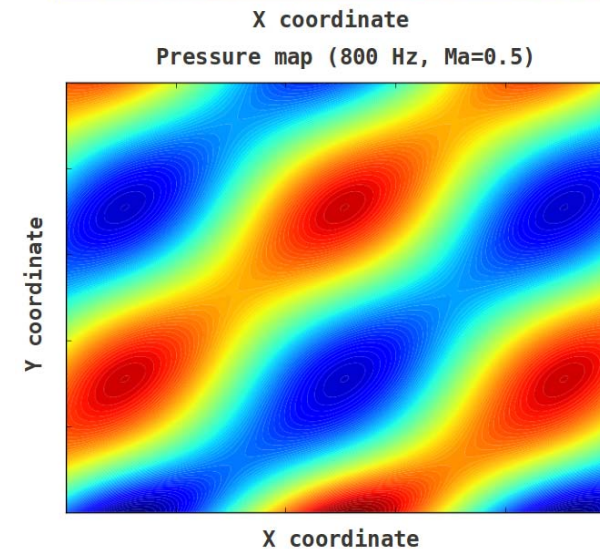
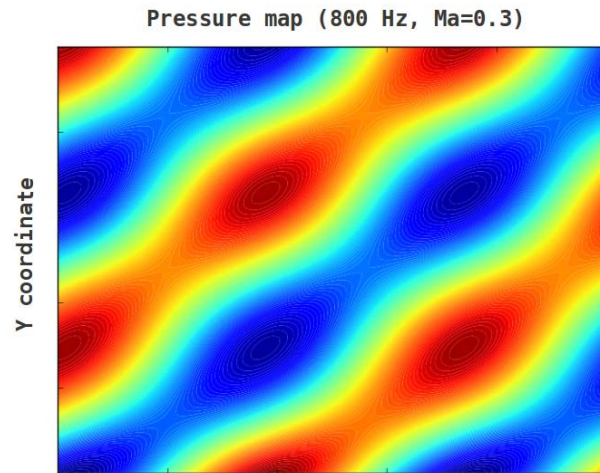


RBLT

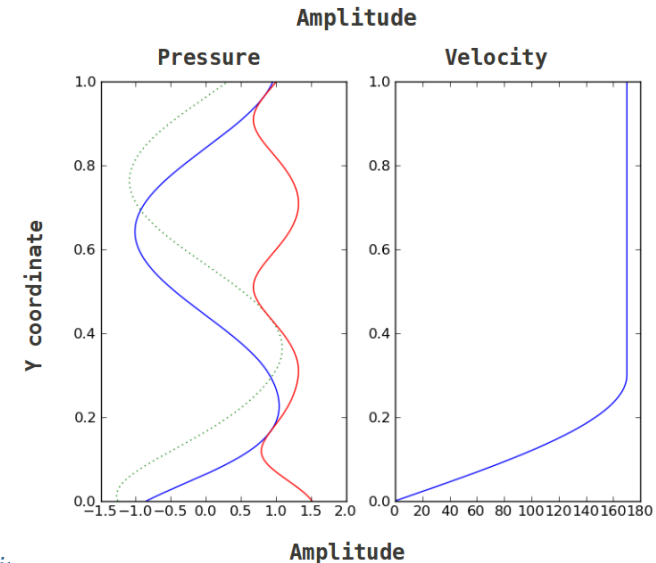


Numerical results (potential model)

➔ Potential operator (Actran TM):

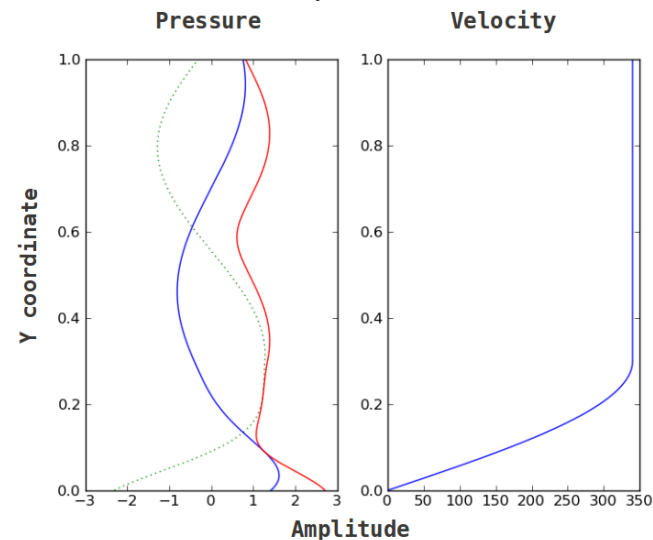
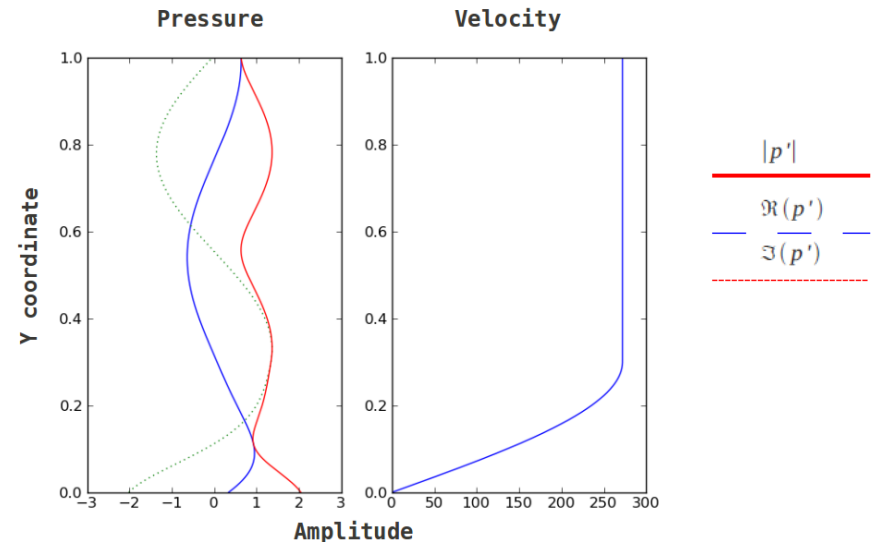
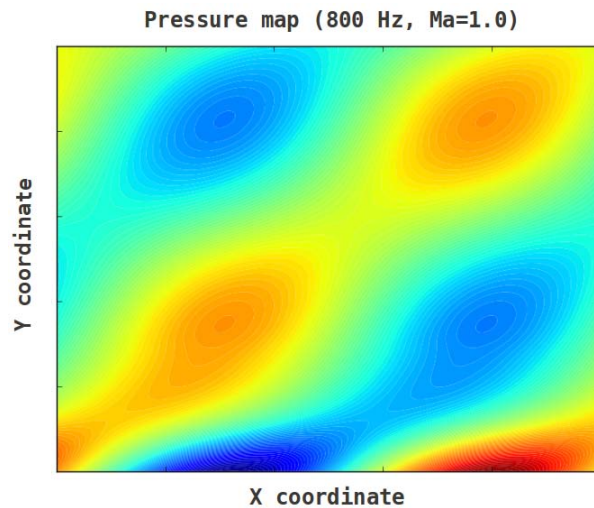
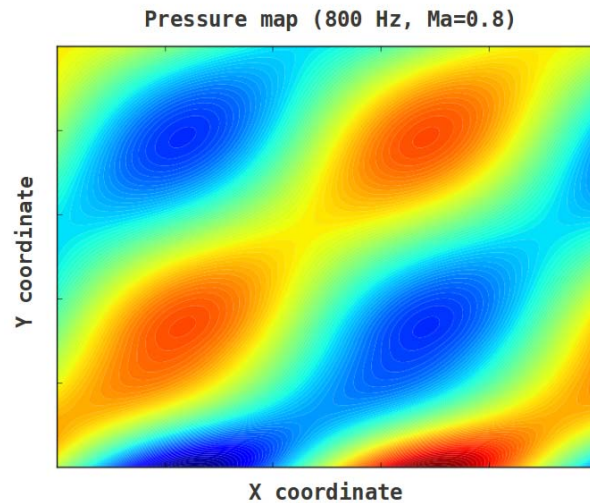


$$\begin{aligned} & |p'| \\ & \Re(p') \\ & \Im(p') \end{aligned}$$



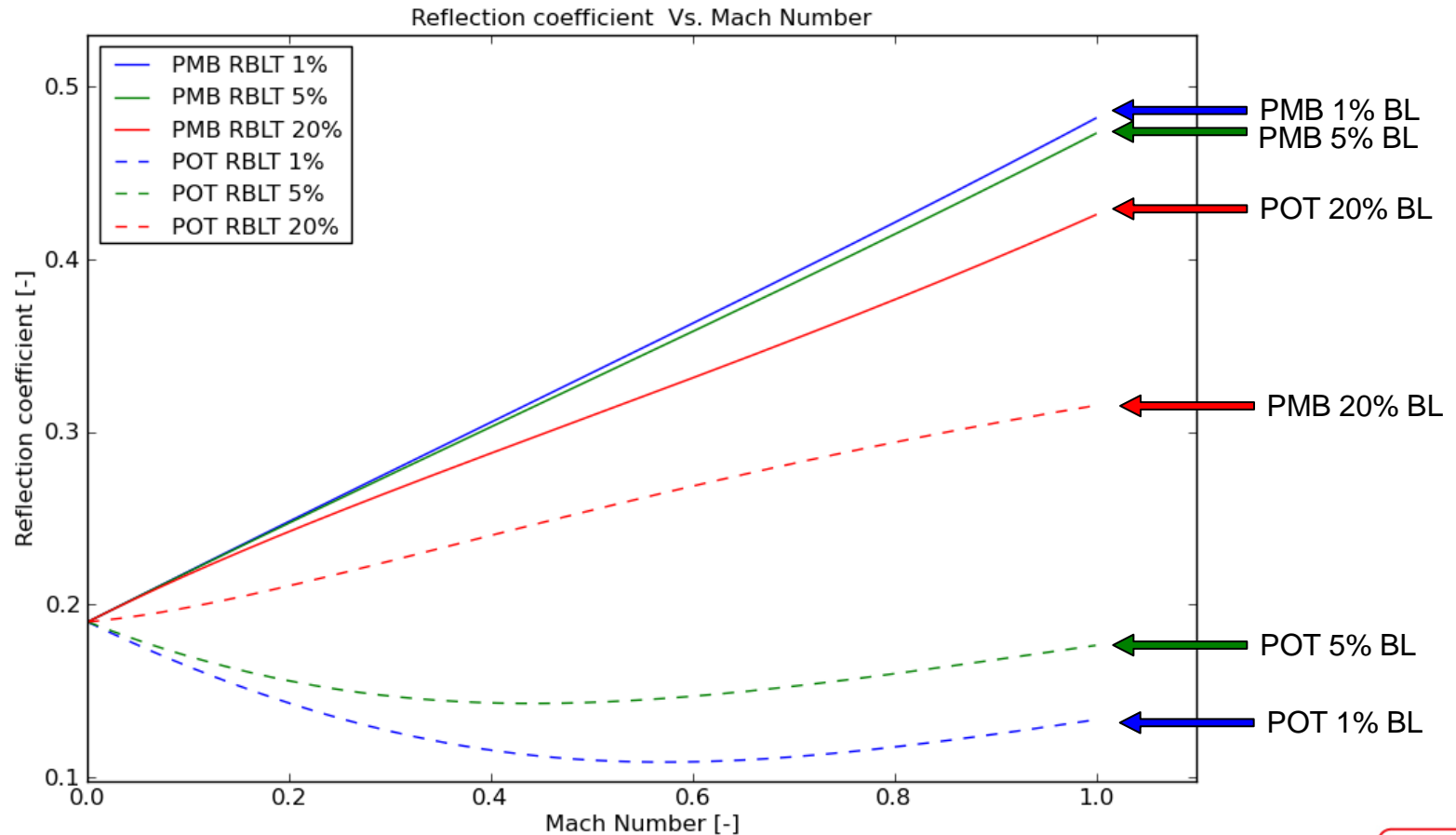
Numerical results (potential model)

➔ Potential operator (Actran TM):



Numerical results (potential model vs. PMB)

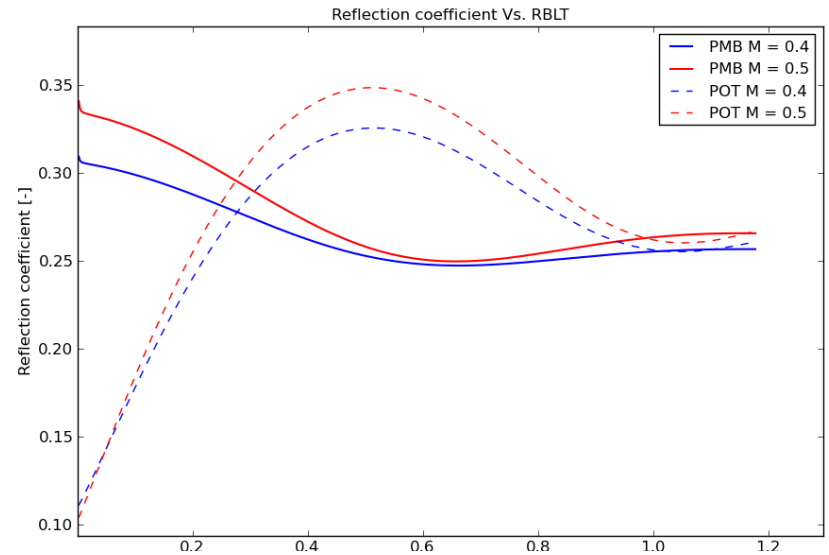
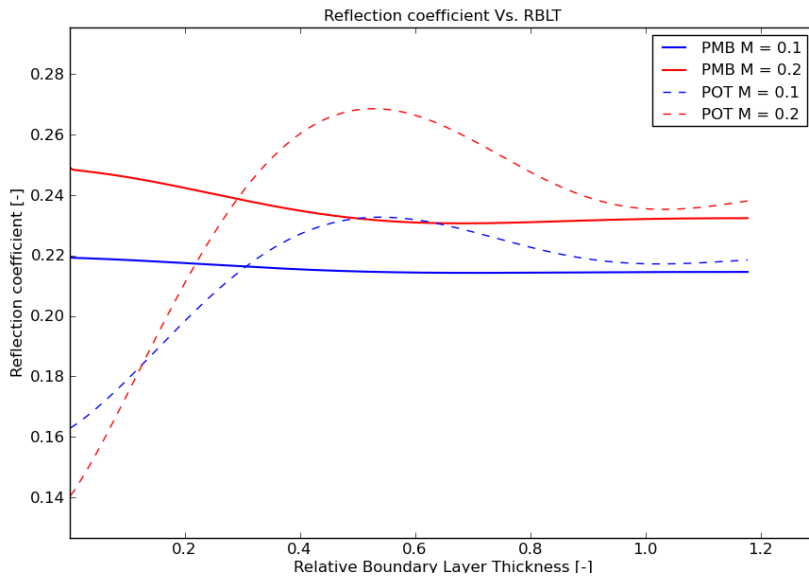
➤ Potential operator: Reflection coefficient vs. Mach number



Numerical results (potential model vs. PMB)

➤ Potential flow operator: Reflection coefficient vs. RBLT

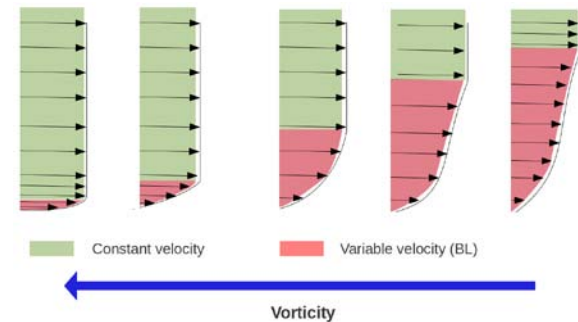
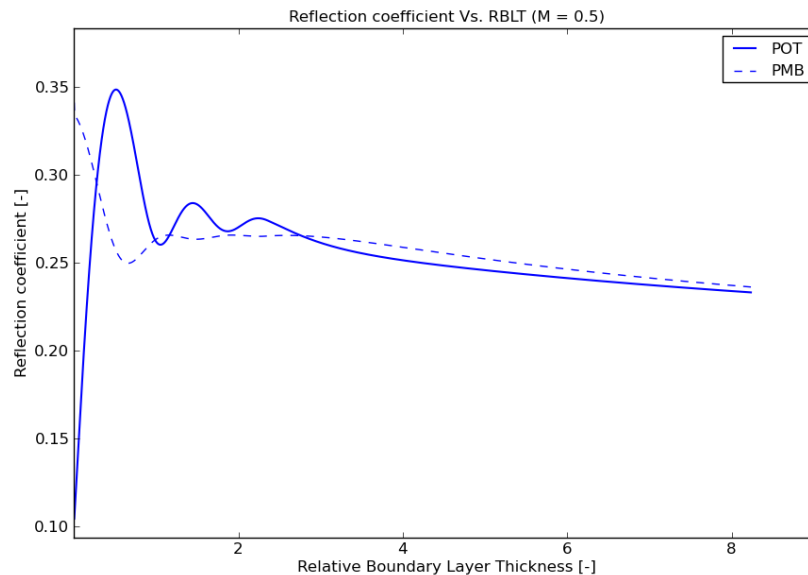
Good behaviour at high RBLT
(Low and medium vorticity)



Numerical results (potential model vs. PMB)

➔ Evaluation of potential operator:

➔ Reflection coefficient vs. RBLT (800 Hz):

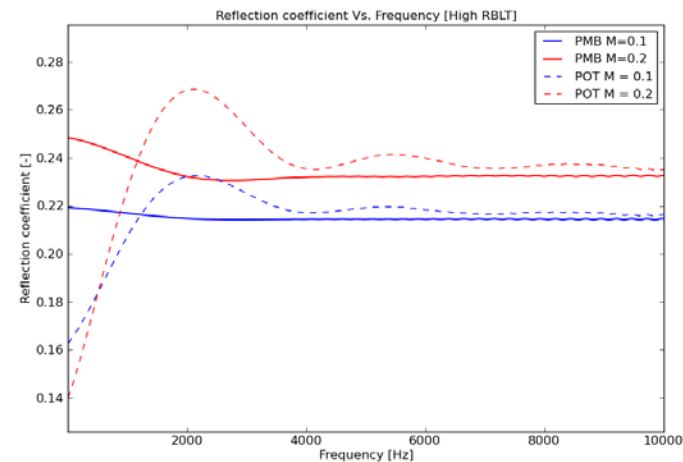
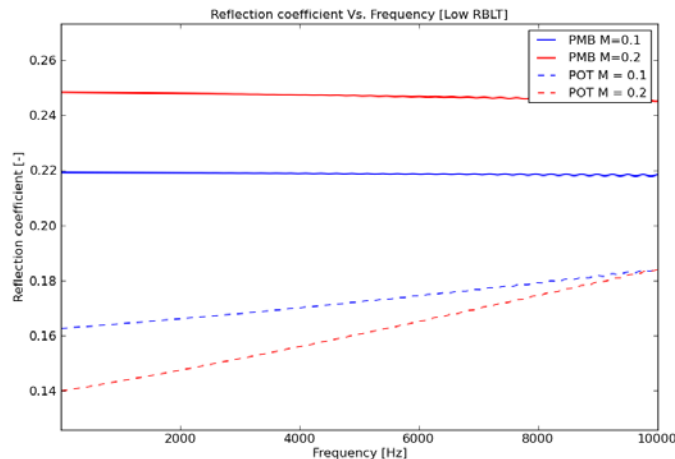
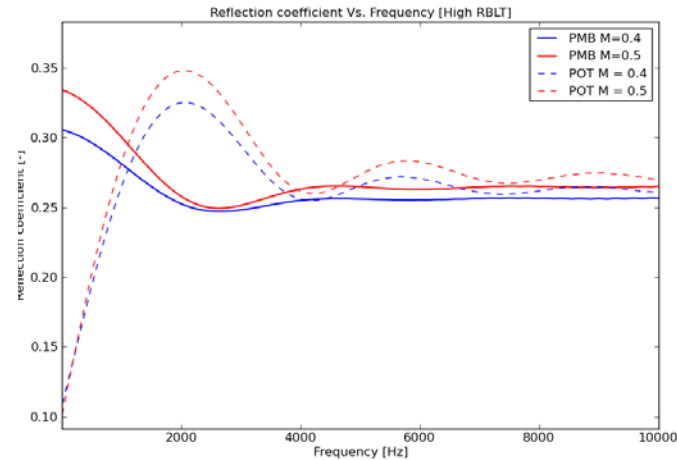
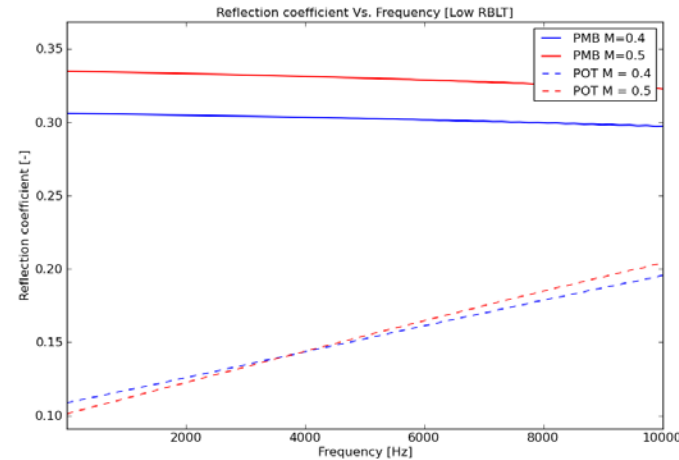


- ➔ If RBLT value is high (i.e. low vorticity), potential model and Pridmore-Brown model give the same results

Numerical results (potential model vs. PMB)

➤ Potential operator: Reflection coefficient vs. frequency

Mach Number



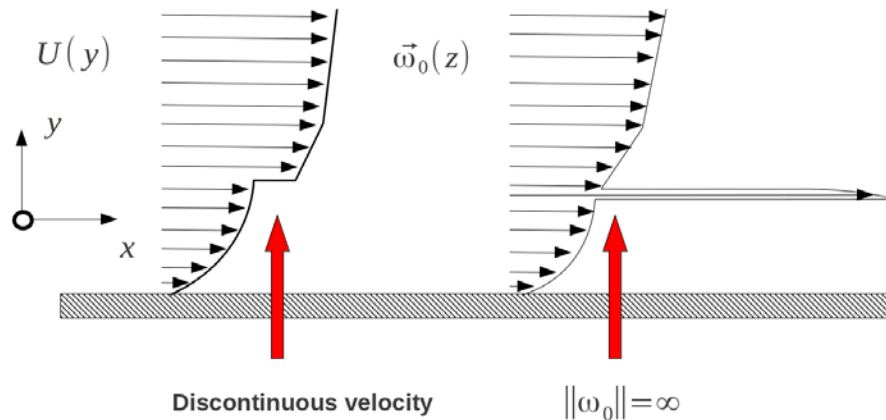
Good behaviour at high frequency

RBLT

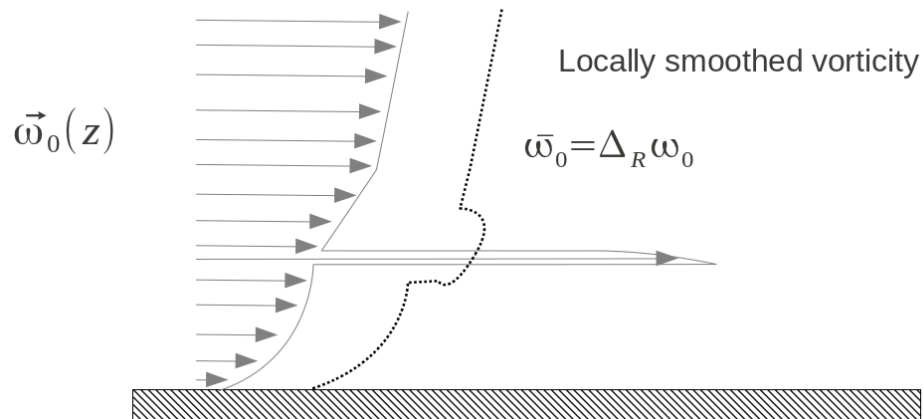


(Extended) Mohring model with regularization

➤ Instability of pressure with flow vorticity



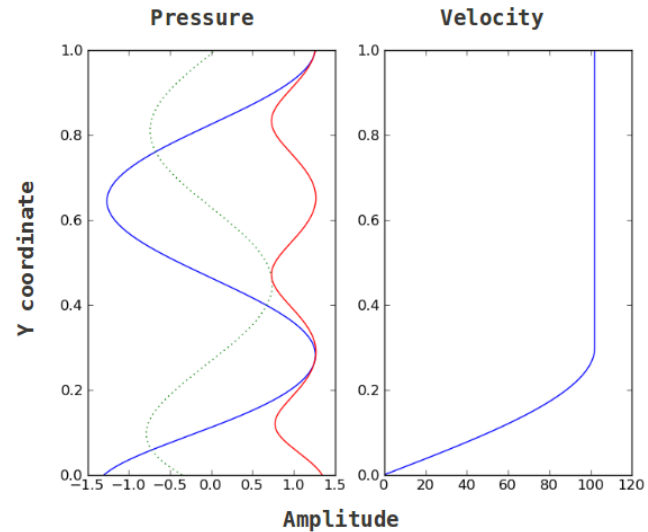
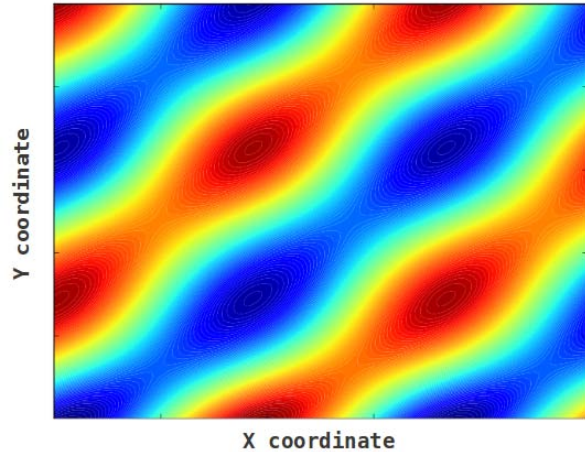
➤ Regularization procedure: smooth high vorticities ...



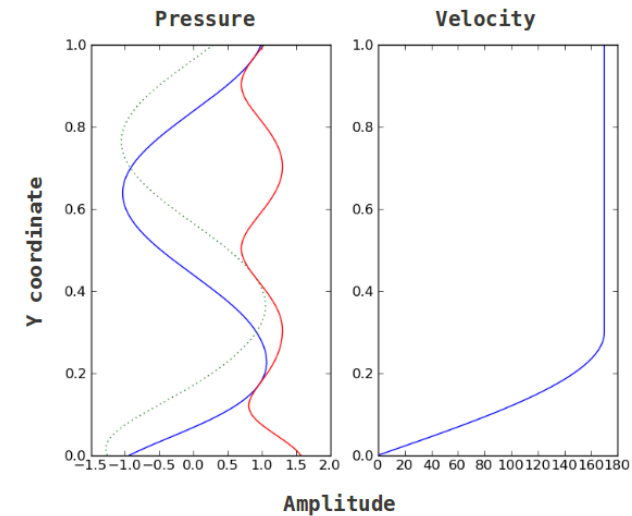
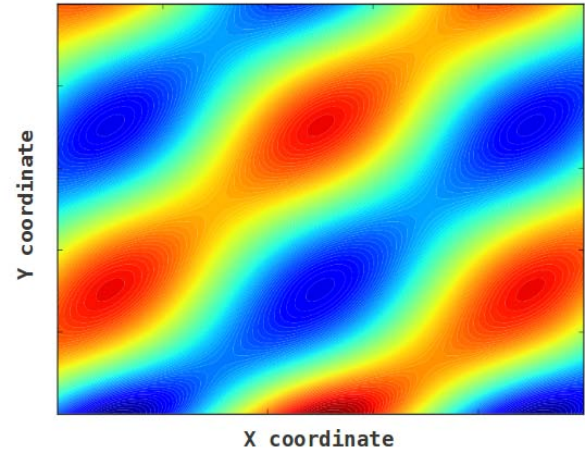
Numerical results (Möhring)

➔ New Möhring equation MOH3R :

Pressure map (800 Hz, $Ma=0.3$)

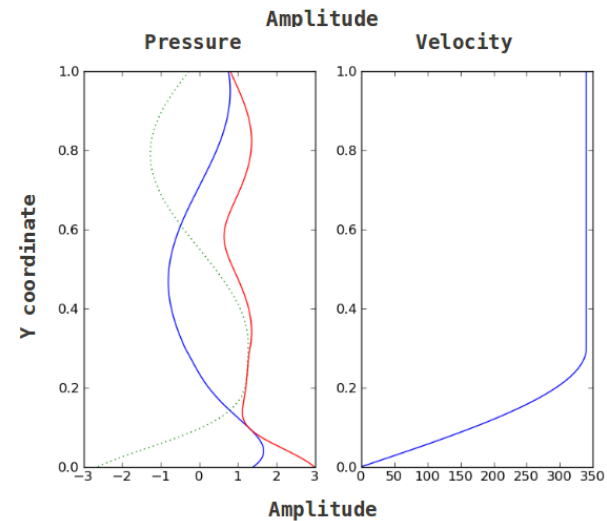
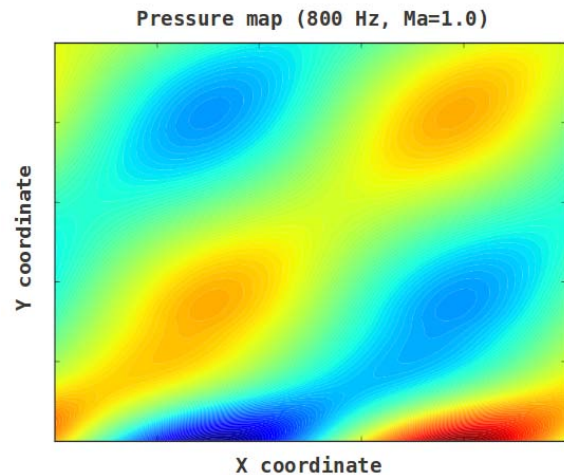
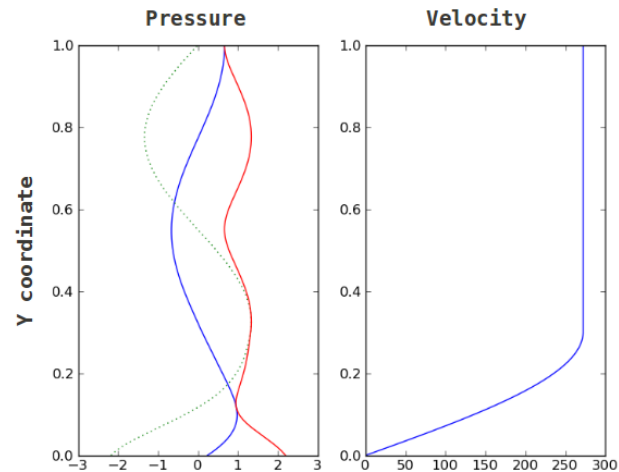
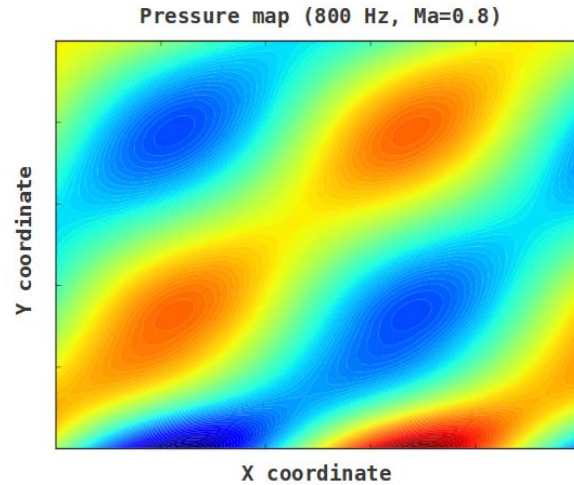


Pressure map (800 Hz, $Ma=0.5$)



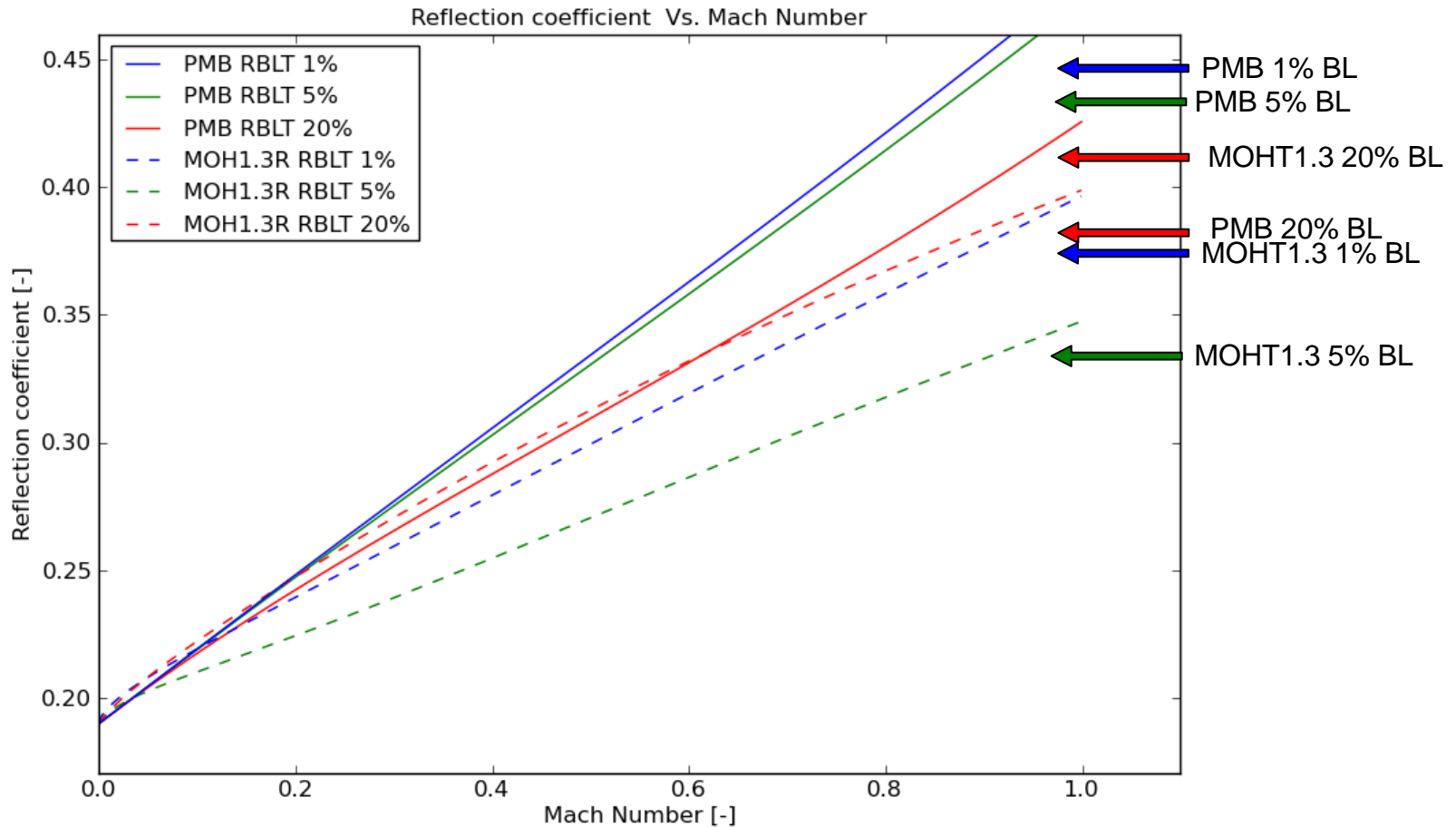
Numerical results (Möhring)

➔ New Möhring equation MOH3R :



Numerical results (Möhring vs. PMB)

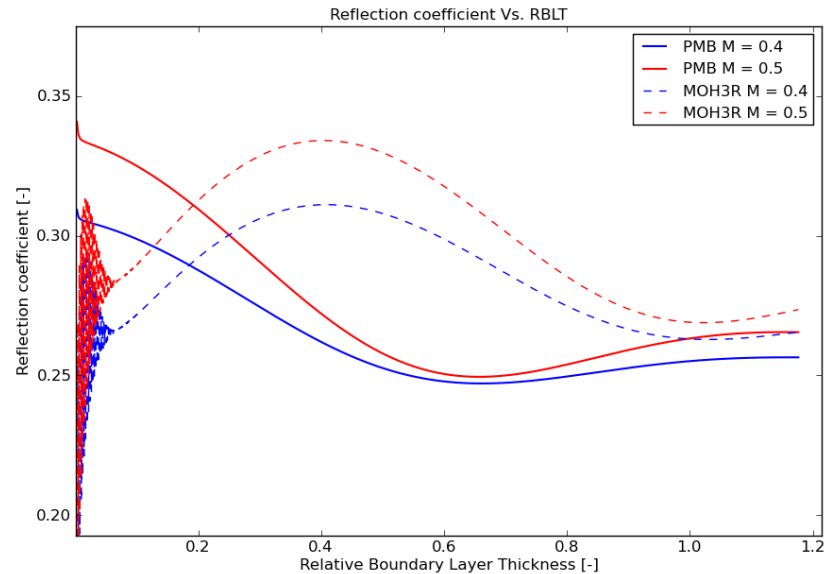
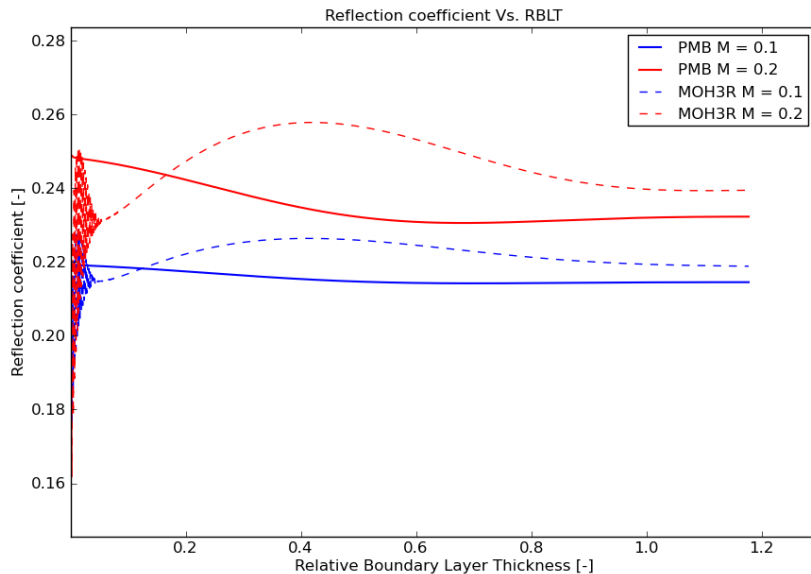
➤ New Möhring equation MOH3R: Reflection coefficient vs. Mach number



Numerical results (Möhring vs. PMB)

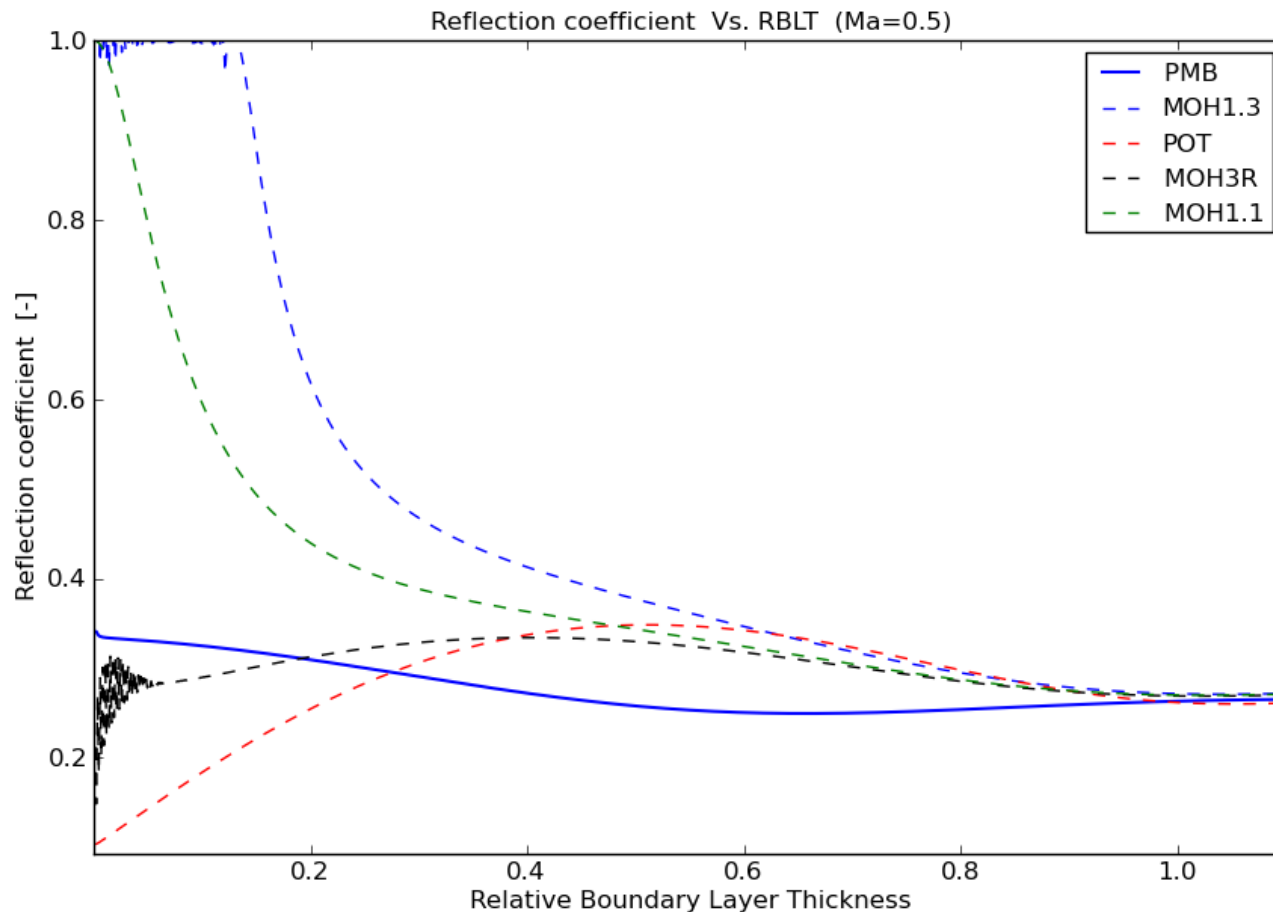
➤ New Möhring equation MOH3R: Reflection coefficient vs. RBLT

Good behaviour at high vorticity



Numerical results (all models)

➔ Reflection coefficient vs. RBLT:



Reducing dispersion errors

➔ Dispersion analysis for wave problems:

- Well established results for standard Helmholtz problem (Harari, 1997; Babuska et al., 1999, etc)
- Extension to convected Helmholtz problem is more recent (Astley, Gamallo and Gabard, 2004)

$$k(\alpha, \theta) = \frac{k_0}{1 + M \cos(\theta - \alpha)}$$

$$\theta - \alpha = 0 \rightarrow \lambda_d = \lambda_0(1 + M)$$

$$\theta - \alpha = \pi \rightarrow \lambda_u = \lambda_0(1 - M)$$

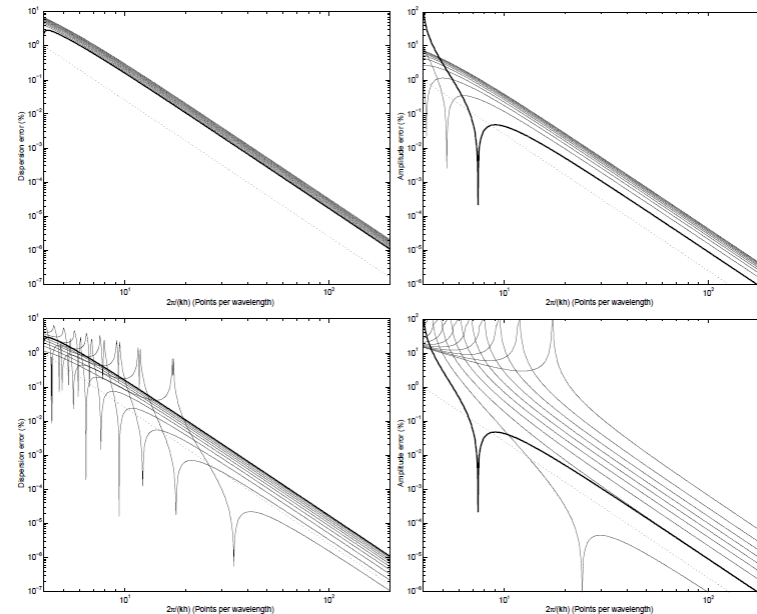
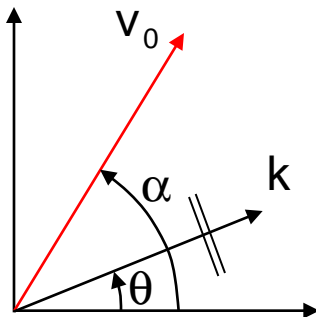


Figure 4: Dispersion error E_d (left) and amplitude error E_a (right), in %, for upstream (top) and downstream (bottom) propagation with the L3, Q8 and Q9 elements. Thick solid line: no flow case ($M = 0$); Solid lines: $M = \pm 0.1$ to ± 0.9 by an increment of 0.1. Dotted line: the fourth order slope.

[Astley et al., ECCOMAS, 2004]



Reducing dispersion errors

➔ Practical ways for reducing dispersion/pollution errors:

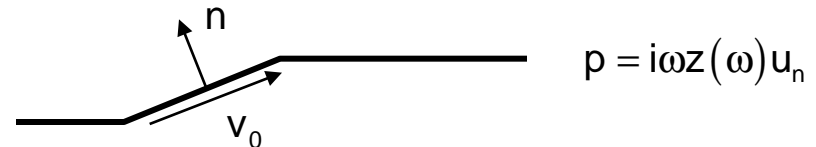
$$\varepsilon_d = \frac{\tilde{k}h - kh}{kh} \quad |\varepsilon_d| \approx C(kh)^{2p}$$

- Higher order polynomials: linear → quadratic → cubic → ...
 - Preserve robustness
 - Compatibility with mesh generators?
- Higher order formulations (partition of unity methods):
 - Plane wave enrichment
 - Ill-conditioning issues → loss of robustness
- Various stabilized formulations ...
 - Example: modified integration schemes (Guddati, 2004)
 - Trivial modification for significant improvements
 - Edge effects (compatibility between modified FE and conventional IE)

Treatment of Myers bc in a FE context

- ➔ Relation between the normal acoustic velocity v_n and the wall displacement u_n in a non-viscous steady flow for harmonic perturbations at frequency ω (Myers):

$$v_n = i\omega u_n + v_0 \cdot \nabla u_n - u_n n \cdot (n \cdot \nabla) v_0$$



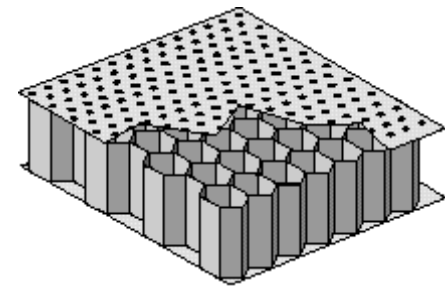
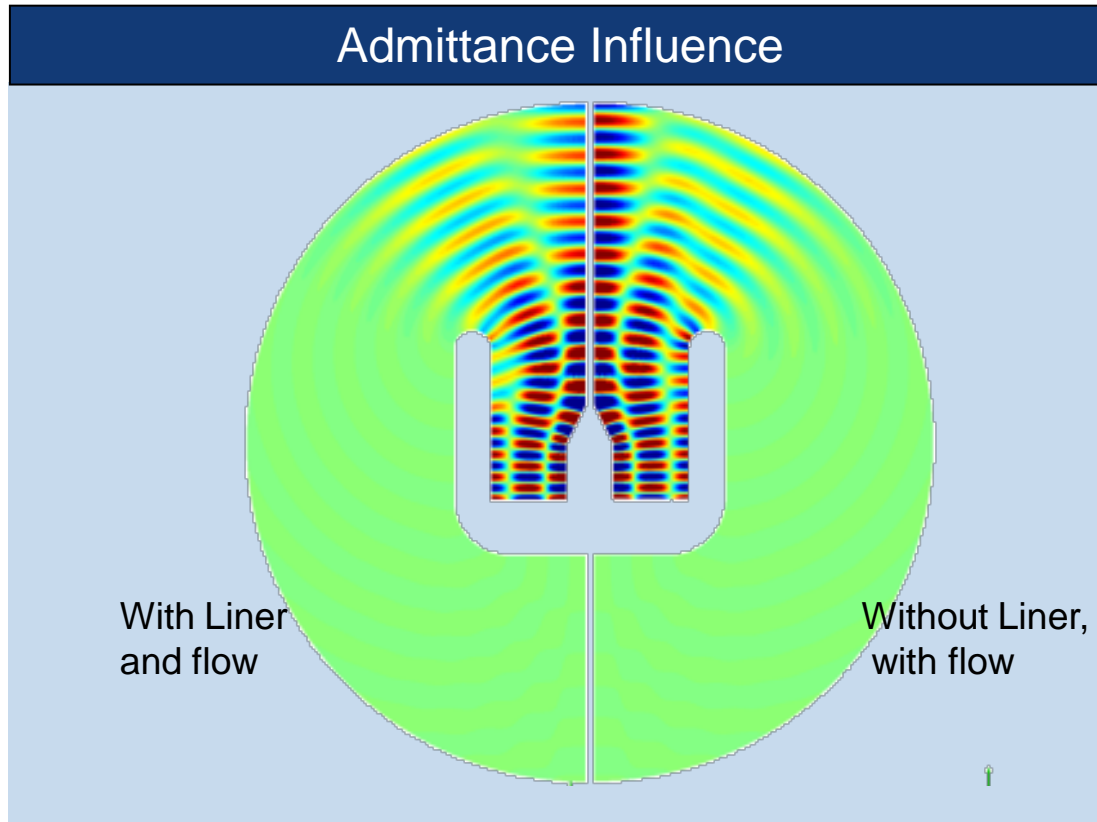
- ➔ Acoustic propagation (in a steady potential flow) based on a velocity potential ϕ

$$\begin{cases} p = -\rho_0 (i\omega\phi + v \cdot \nabla\phi) \\ v = \nabla\phi \end{cases}$$

- ➔ Handling of this boundary condition in a FE context:
 - Main difficulty: velocity derivative in Myers bc leads to involve the second order derivative of the potential
 - Regularization proposed by Eversman (JSV, 2001)

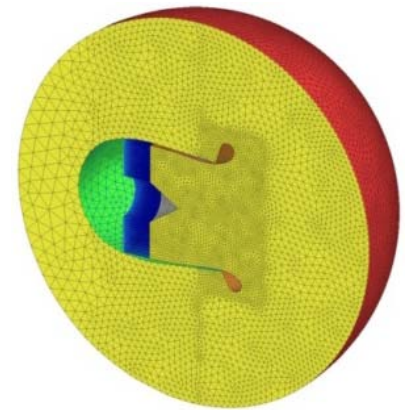
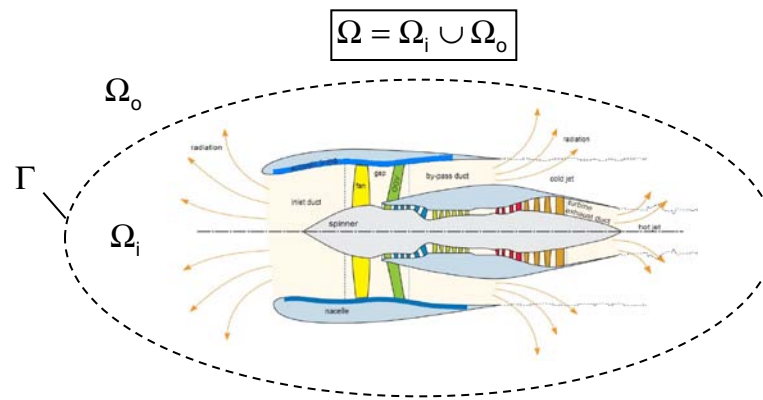
Example / Myers-Eversman boundary condition

- ➔ Actran TM incorporates Eversman regularization technique for handling Myers boundary condition
- ➔ Evaluation of acoustic attenuation provided by liners for flow/non-flow cases



Computational domain

- ➔ Handling the external radiation condition in a domain based formulation
- ➔ Partition of the propagating domain into inner and outer sub-domains:



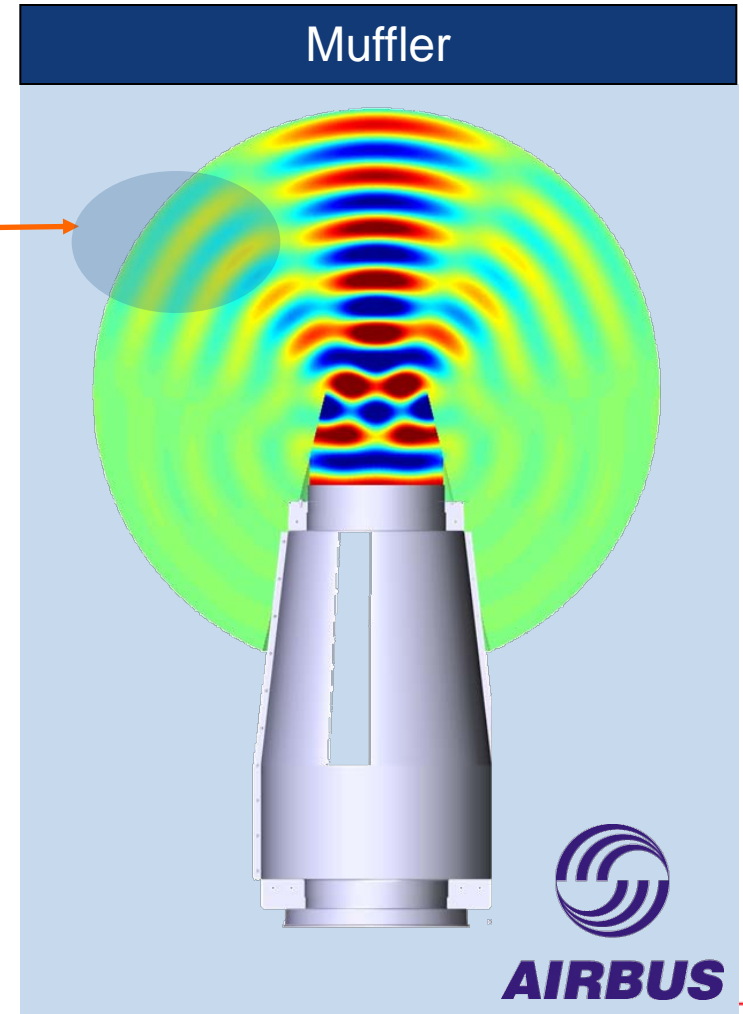
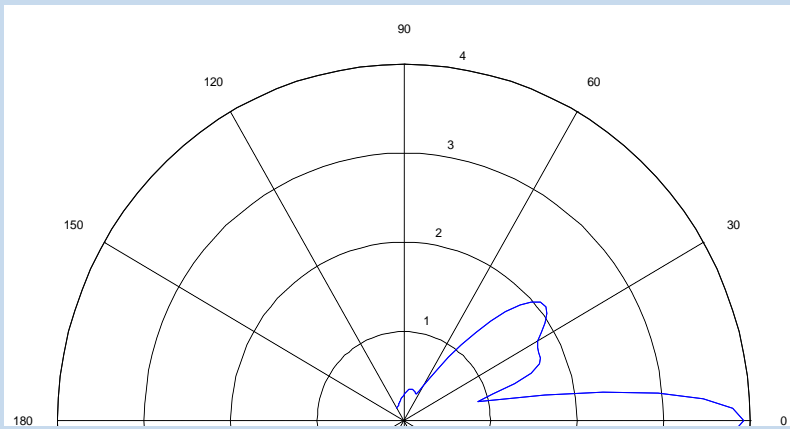
- ➔ Usual technique for handling the outer sub-domain:
 - Infinite elements (Atley-Leis formulation, uniform flow, higher-order radial interpolation scheme) ← Actran TM
 - Buffer zones (« PML ») ← Actran DGM
- ➔ Far field evaluation can rely on boundary integral representations (FWH)

Interest of infinite elements

➔ Two roles:

- Act as a non reflective boundary condition (free field modeling)
- Give access to results outside the inner domain

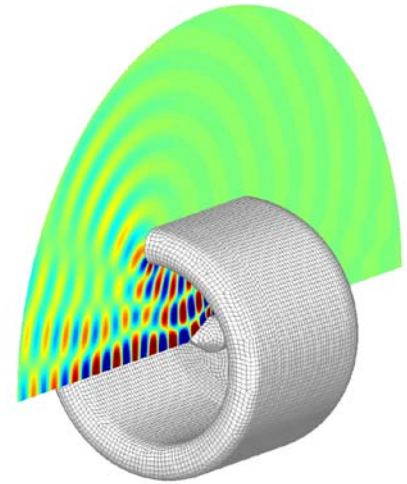
Directivity Diagram



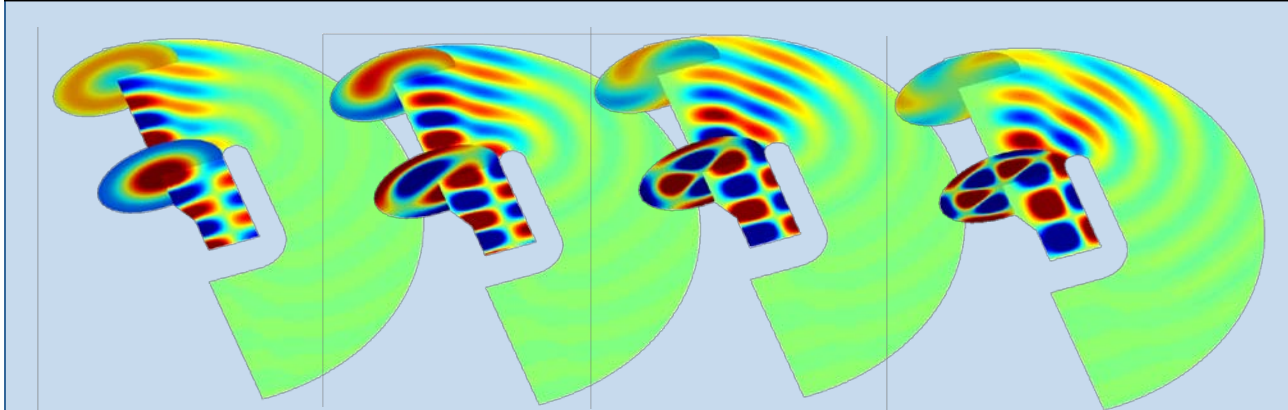
Axisymmetric computations

➔ Axisymmetry features:

- 3D results at (almost) the cost of a 2D computation!
- Meshing is easier
- Post-processing is faster
- Sufficient for early design



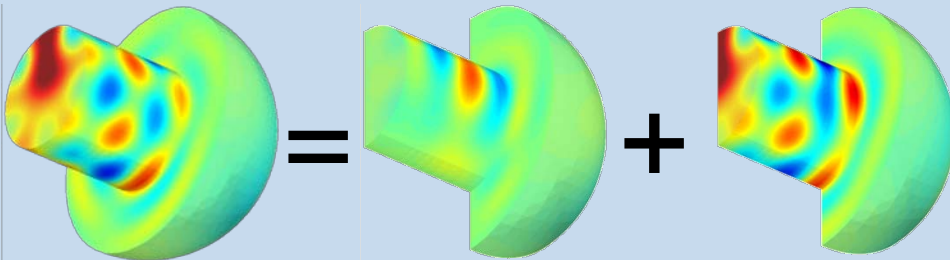
Results for different azimuthal orders



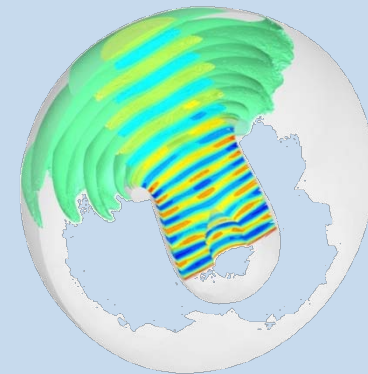
Symmetry & Anti-Symmetry

- ➔ Actran can take advantage of spinning modes decomposition:
 - The 2 half models are based on the same mesh → Same pre-processing time than for the complete model
 - Allows both to improve the performances and to perform computations on large size problems
 - Leads to 4 times less CPU & RAM

Symmetric and anti-symmetric decomposition strategy



Computation on a half nacelle



Modal ducts

➔ Modal ducts:

- Acoustic propagation in cylindrical ducts:

$$\Delta_{xy}\phi + (1-M^2)\frac{\partial^2\phi}{\partial z^2} - 2ikM\frac{\partial\phi}{\partial z} + k^2p = 0$$

- Solution in terms of transverse modes:

$$\phi(x, y, z) = \sum_{m,n} \phi_{mn}(x, y) \left(a_{mn}^+ e^{-ik_{zmn}^+ z} + a_{mn}^- e^{-ik_{zmn}^- z} \right)$$

- Available cross-section geometries:
 - Circular, annular and rectangular → analytical formulation
 - Arbitrary → numerical formulation
- Cut-on frequencies related to identified modes
- Modal intensity

➔ Coupling FE model with a modal duct component:

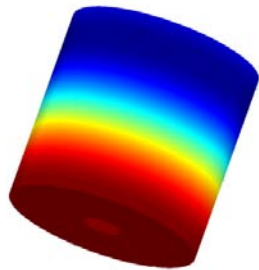
- Mixing physical and modal unknowns in the underlying variational form
- Possibility to constraint individual modes
- Driving modes in amplitude or intensity

➔ Application to broadband fan noise through modal energy equirepartition



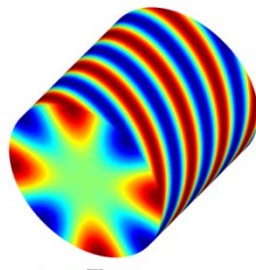
Modeling sources using duct modes

- ➔ Source represented by a set of duct modes (Tyler & Sofrin theory)
- ➔ These modes are rotating modes characterized by with radial and azimuthal orders
- ➔ Selection of constrained modal amplitudes can rely on well established rules
- ➔ Reflected modes are let free (non reflecting boundary condition)



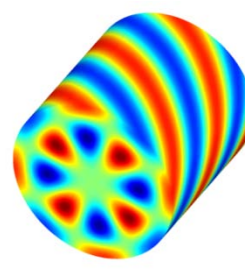
Radial order = 1

Azimuthal order = 0



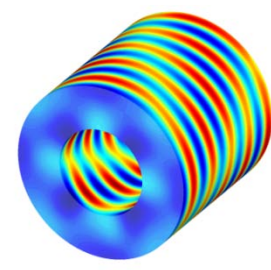
Radial order = 1

Azimuthal order = 4



Radial order = 2

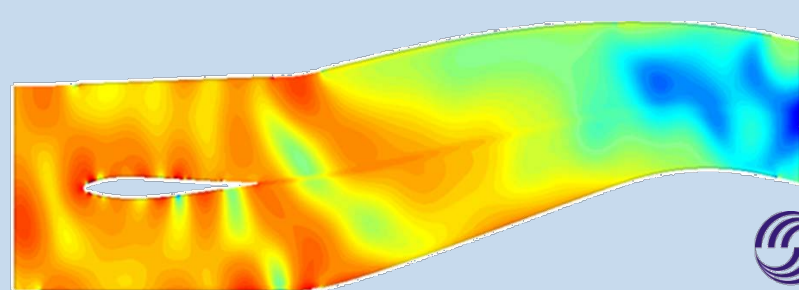
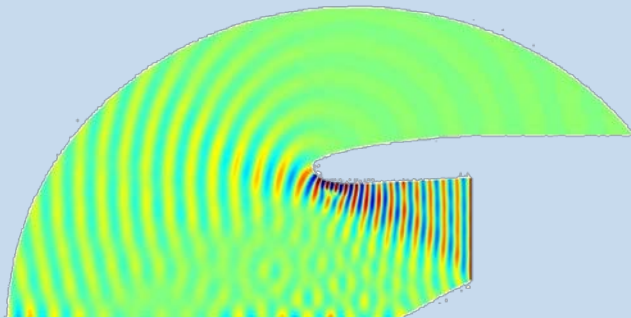
Azimuthal order = 4



Radial order = 3

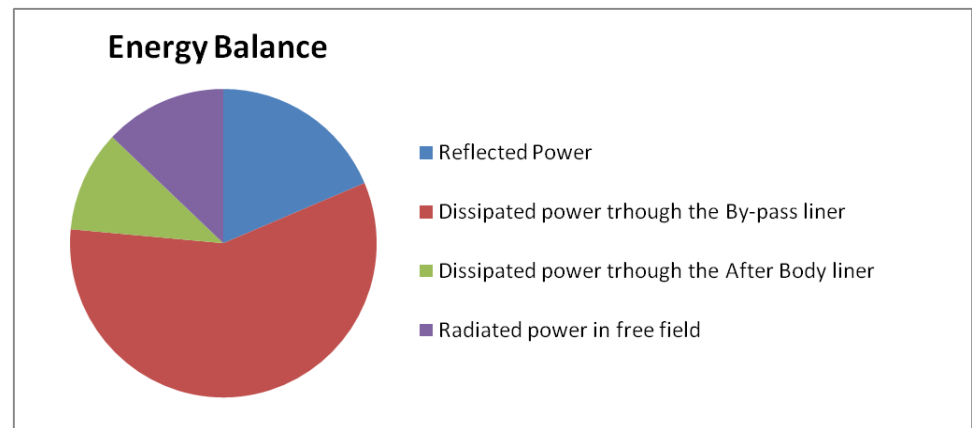
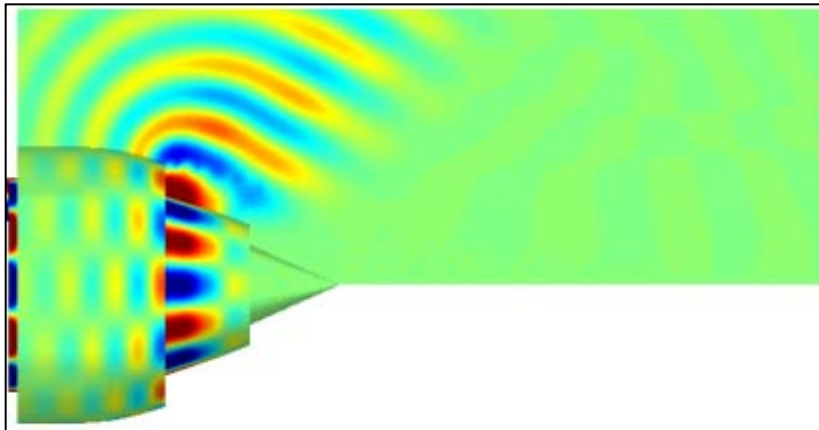
Azimuthal order = 4

Axisymmetric Nacelle & Splitter in a Bypass



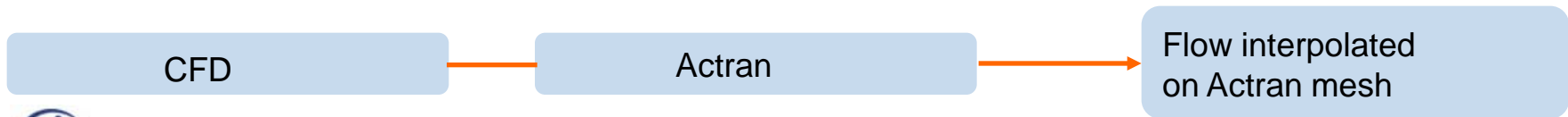
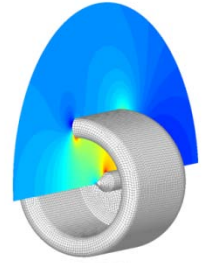
Capability to produce relevant indicators

- ➔ Output maps for near field and far field
- ➔ Directivity diagrams
- ➔ Energy indicators → energy balance of the system

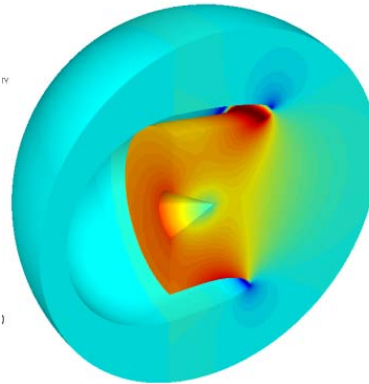


Handling the mean Flow

- ➔ Actran TM can handle heterogeneous mean flow
- ➔ A compressible potential flow calculation can be performed
- ➔ Alternative: use an external CFD code
 - Coupling with Star-CD, Fluent and other proprietary codes
 - Procedure:

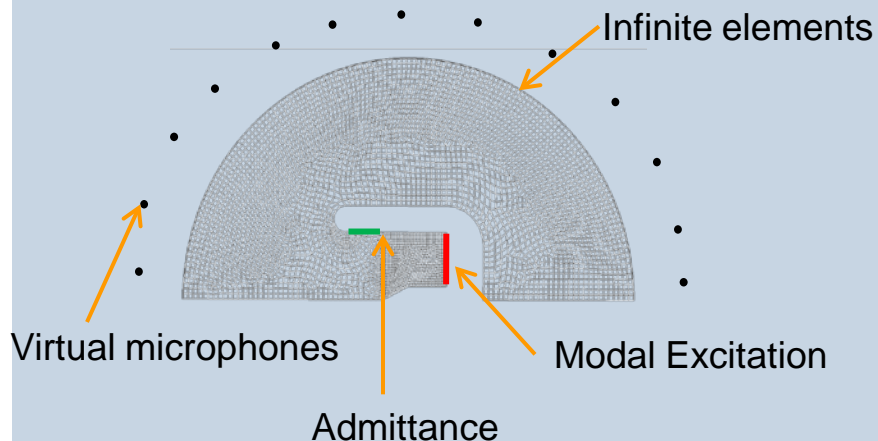


FLUENT

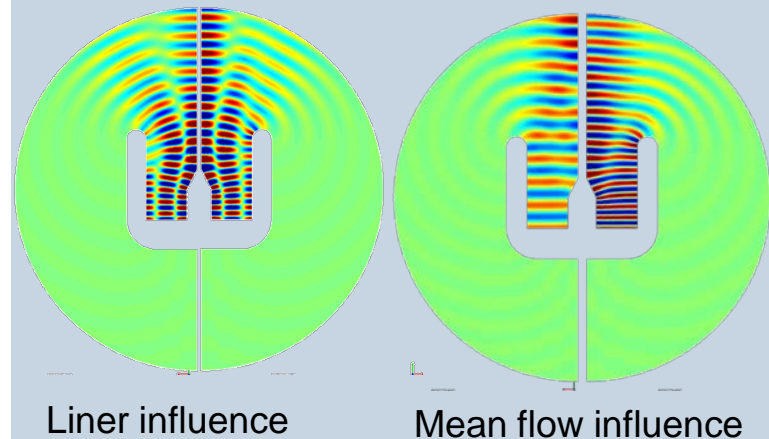


Case Study: Nacelle Inlet

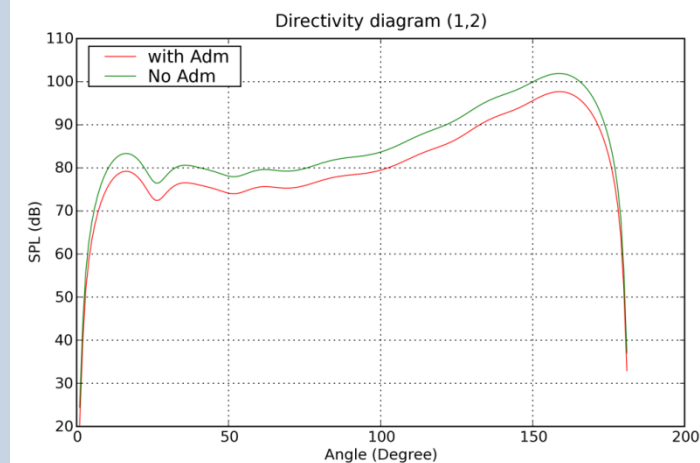
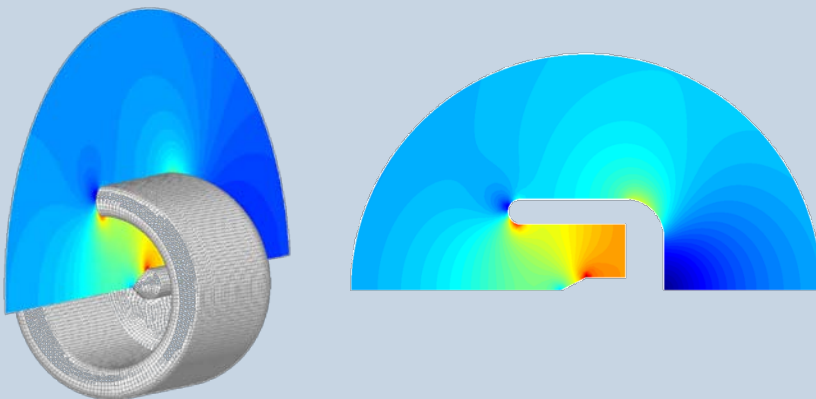
ACTRAN model



Results

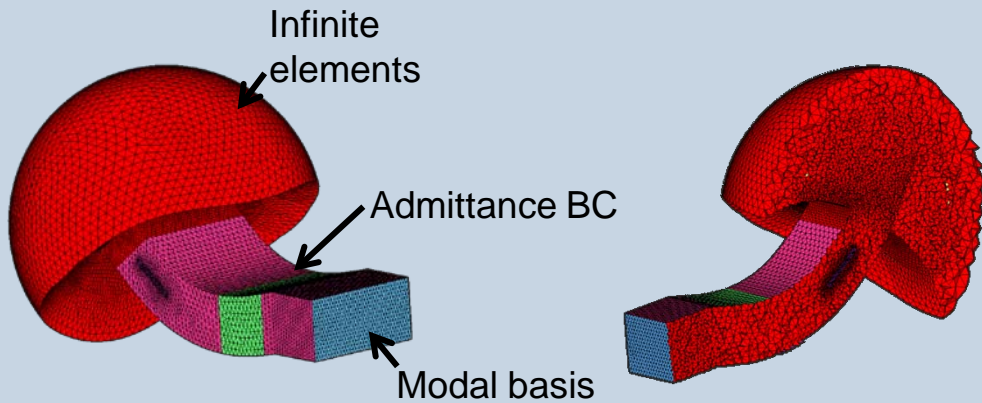


Mean flow computed with ACTRAN

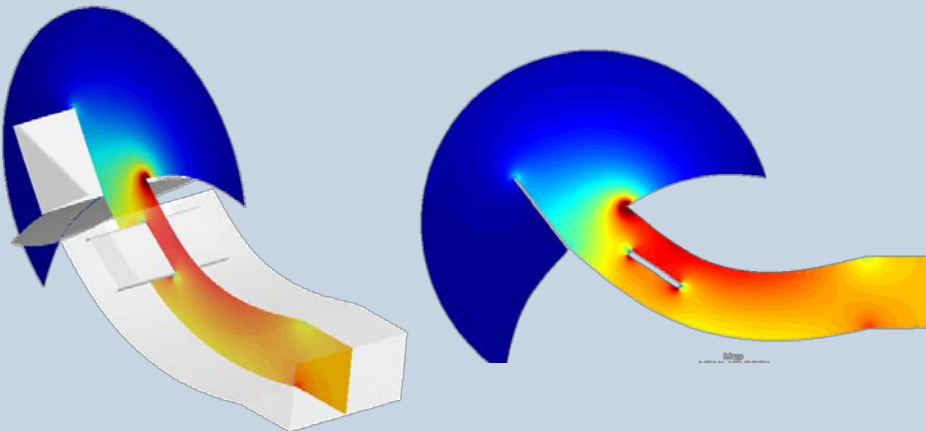


Case Study: APU

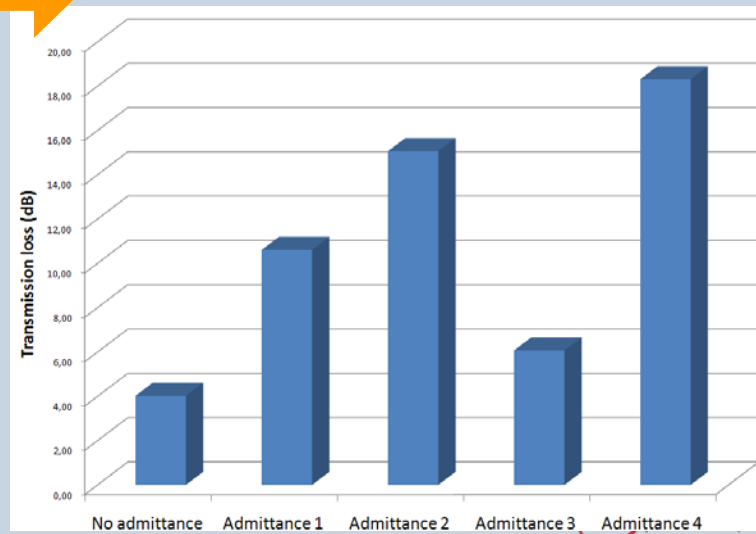
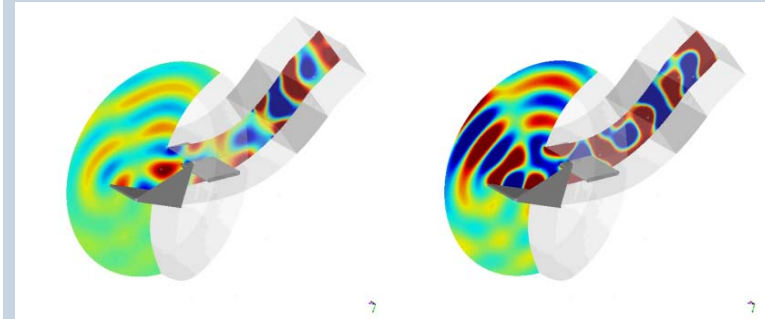
ACTRAN Model



Mean flow computed by Fluent



Results



Experimental validations

- ➔ Many investigators have performed experimental validations
- ➔ Some earlier works:
 - "Fan Noise Radiation from Intake: Comparisons between FEM Prediction and Fan Rig Test Measurements with Flare", S.Lidoine & B.Caruelle, ICSV 2005

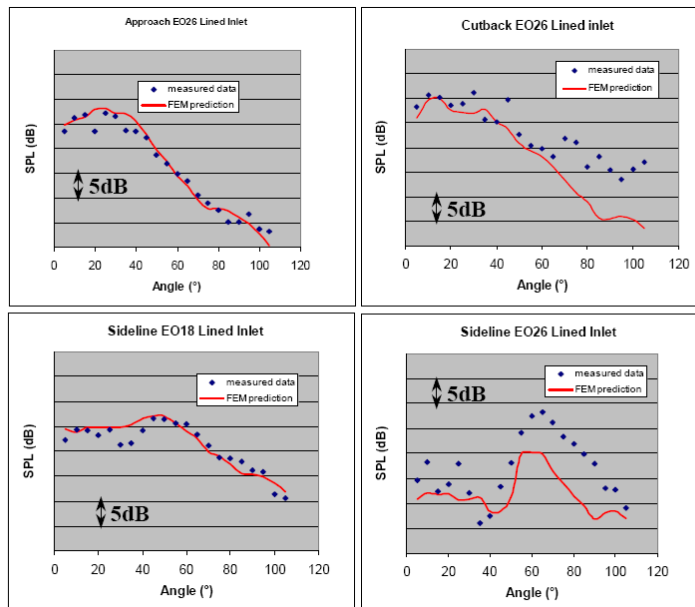


Figure 6 – Comparisons between measured data and ACTRAN prediction, Lined inlet case.

- "Development and validation of a parallel out-of-core propagation and radiation code with validation on a turbofan application", P.Ploumhans et al, ICA 2004-702



Parallelisms & Multi-Loadcase

➔ Domain parallelism

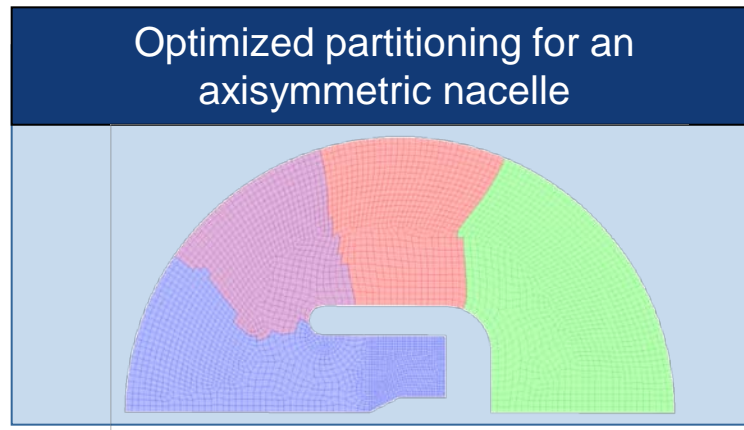
- Improves the computation performances (scalability)
- Allows to perform computations on large models
- Automatic optimized partitioning

➔ Frequency parallelism

- Computations at several frequencies are performed at the same time
- (Perfect) scalability

➔ Multi-loadcase capability

- All modal responses computed in one computation
- Mandatory for broadband computations



Solver efficiency

➔ Airbus tests (A. Mosson, User's meeting, 2010):

Radiating Inlets with ACTRAN/TM

- Objectives
 - To define optimal run parameters
 - To evaluate the highest frequency reachable on our clusters

- Release

- Actran_10.0

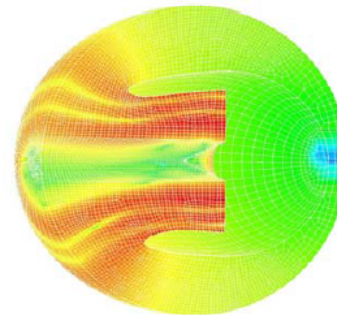
- Description

- A380 T900 3D inlet
 - 3 different $\frac{1}{2}$ models
 - Hybrid mesh (hexa, pyra, penta, tetra)
 - Broad band calculation

- Run parameters

- MPI parallelism
 - Multithreading
 - In/out-of core MUMPS solver
 - Right Hand Side (RHS) Block Size

Frequency	0.5 bpf	1 bpf	2 bpf
Kdofs	412	2059	7047
Cut-on modes	41	147	578

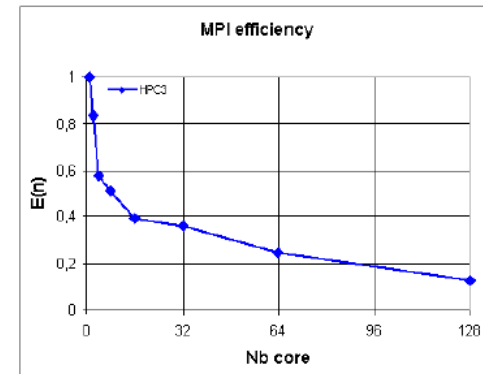
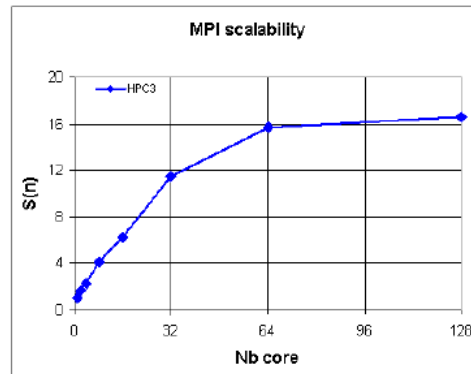
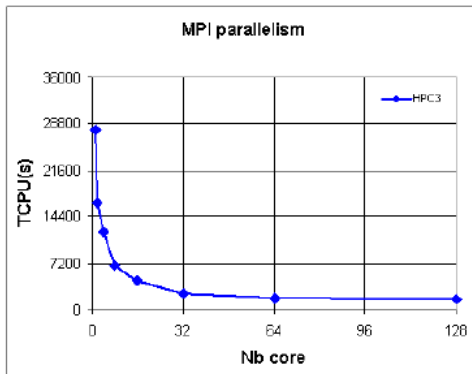


Solver efficiency

➔ Airbus tests (A. Mosson, User's meeting, 2010):

MPI Parallelism and Multithreading Efficiency

- MPI parallelism
 - 1bpf model
 - In-core MUMPS Solver
 - Single load simulation



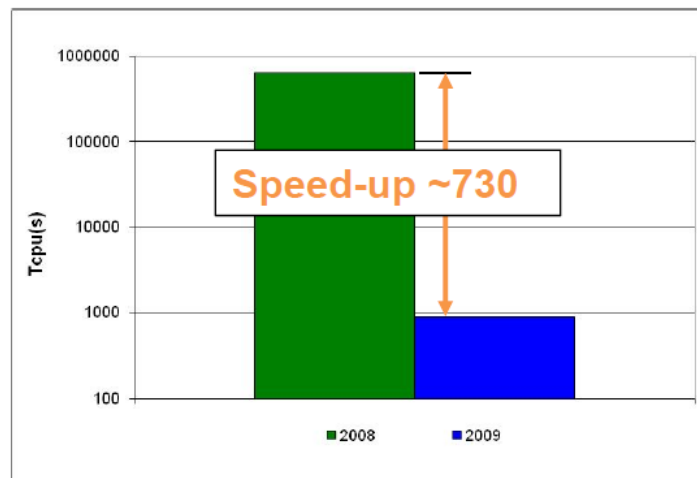
- Interesting scalability up to 64 cores
- The efficiency remains quite good up to 32 cores

Solver efficiency

➔ Airbus tests (A. Mosson, User's meeting, 2010):

Improvement since 2008

- 1bpf model – Single load simulation



- Power 5+ to Nehalem architecture ⇒ **Speed-up ~ 2.5**
- SPARSE to MUMPS solver ⇒ **Speed-up ~ 9**
- Optimal parallelism 32 mpi x 4 threads ⇒ **Speed-up ~ 32**

Conclusions

- ➔ Overview of key ingredients for modeling flow acoustic problems:
 - Availability of various propagation models
 - Modeling liners and handling shear layer effects
 - Exterior acoustics for domain based formulations
 - Modal coupling for handling excitations
 - Relevant output indicators
 - Performance issues:
 - Axi-symmetric vs. 3D models
 - Symmetric/anti-symmetric decomposition
 - Parallelism
 - Solver efficiency

Challenges

- ➔ Establish links between sub-models (example: DNS for $z(\omega)$ → CWE for response)
- ➔ Develop and implement criteria to secure the selection of appropriate reduced models
- ➔ Develop and implement a posteriori error indicators
- ➔ Develop robust higher-order formulations for the short wave problem
- ➔ Investigate appropriate strategies for modeling bulk reacting liners
- ➔ Improve solver performances (a continuous process!)

Thanks to our customers!



GE
Aviation



GE Global Research
United States - India - China - Germany

Honeywell

